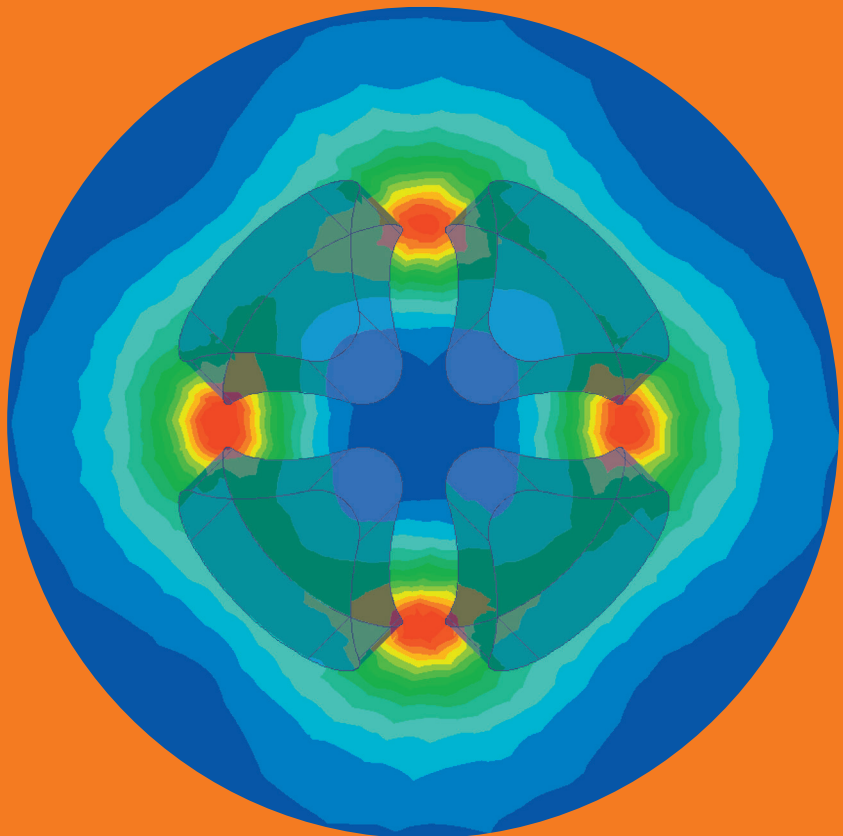


Department of Radio Science and Engineering

# Metamaterials for optical and THz ranges: design and characterization

---

Dmitry Morits



# Metamaterials for optical and THz ranges: design and characterization

**Dmitry Morits**

A doctoral dissertation completed for the degree of Doctor of Science in Technology to be defended, with the permission of the Aalto University School of Electrical Engineering, at a public examination held at the lecture hall S1 of the school on 3 June 2014 at 12.

**Aalto University**  
**School of Electrical Engineering**  
**Department of Radio Science and Engineering**

**Supervising professor**

Prof. Constantin Simovski

**Preliminary examiners**

Prof. Andrea Alù, The University of Texas at Austin, Austin, TX, U.S.A.

Prof. Didier Lippens, Université des Sciences et Technologies de  
Lille, Lille, France

**Opponent**

Prof. Gennady Shvets, The University of Texas at Austin, TX, U.S.A.

Aalto University publication series

**DOCTORAL DISSERTATIONS** 55/2014

© Dmitry Morits

ISBN 978-952-60-5658-6

ISBN 978-952-60-5659-3 (pdf)

ISSN-L 1799-4934

ISSN 1799-4934 (printed)

ISSN 1799-4942 (pdf)

<http://urn.fi/URN:ISBN:978-952-60-5659-3>

Unigrafia Oy  
Helsinki 2014

Finland



**Author**

Dmitry Morits

**Name of the doctoral dissertation**

Metamaterials for optical and THz ranges: design and characterization

**Publisher** School of Electrical Engineering

**Unit** Department of Radio Science and Engineering

**Series** Aalto University publication series DOCTORAL DISSERTATIONS 55/2014

**Field of research** Radio Engineering

**Manuscript submitted** 13 March 2014

**Date of the defence** 3 June 2014

**Permission to publish granted (date)** 2 April 2014

**Language** English

**Monograph**

**Article dissertation (summary + original articles)**

**Abstract**

The thesis is devoted to the field of metamaterials (MtMs) - effectively continuous artificial composites with advantageous electromagnetic properties not normally met in nature. The main goal of the work is the engineering of MtMs with new and extreme electromagnetic properties and their electromagnetic characterization.

The first part of the thesis is focused on the artificial magnetism and isotropic negative permittivity and permeability in the near-infrared and visible ranges. Several design solutions based on resonant complex-shaped inclusions are proposed and studied analytically and numerically. In the first design utilization of clusters of plasmonic dimers leads to the negative permeability in the near-infrared range. Next suggested MtM consisting of the clusters of plasmonic triangular nanoprisms possesses isotropic negative permeability on the boundary between the near-infrared and visible ranges. The third design based on core-shell metal-dielectric particles allows for the isotropic negative refractive index in the near-infrared range.

The second part of the thesis is devoted to the problem of characterization of planar and bulk MtMs. At first, the applicability of the so-called Holloway-Kuester method is studied for the planar arrays of complex inclusions. It is shown, that despite the fact that the approach initially was developed for the arrays of solid particles in the quasi-static approximation, it is also applicable for the arrays of rather optically substantial resonant clusters of plasmonic nanoparticles. Then, the method of homogenization of bulk MtMs is suggested, based on the account of electromagnetic interaction between crystal planes forming an orthorhombic lattice. The method reveals the electromagnetic properties not covered by the standard quasi-static homogenization procedures.

The last research problem studied in the thesis is the engineering of planar multifunctional MtMs for the THz range. The suggested MtM consists of resonant metal stripes put on both sides of an elastic polymer film and allows for the combination of polarization transformation properties with sensitivity to the applied strain. The design is studied theoretically, numerically, and experimentally. For the last purpose an original fabrication method is developed, allowing for the rather simple creation of optically large samples. The fabricated sample experimentally demonstrates a high sensitivity to stretching in the transmission coefficient for the co-polarized field.

**Keywords** metamaterials, metasurfaces, plasmon resonance, artificial magnetism, characterization

**ISBN (printed)** 978-952-60-5658-6

**ISBN (pdf)** 978-952-60-5659-3

**ISSN-L** 1799-4934

**ISSN (printed)** 1799-4934

**ISSN (pdf)** 1799-4942

**Location of publisher** Helsinki

**Location of printing** Helsinki

**Year** 2014

**Pages** 114

**urn** <http://urn.fi/URN:ISBN:978-952-60-5659-3>



# Preface

The doctoral thesis has been carried out in the Department of Radio Science and Engineering at Aalto University, School of Electrical Engineering. My warmest gratitude goes to my supervisor, Prof. Constantin Simovski, for his guidance and support during this research. I would also like to thank Prof. Sergei Tretyakov for fruitful discussions and sharing his experience in the field of metamaterials.

I am grateful to the present and former members of our scientific group: Dr. Igor Nefedov, Dr. Pekka Alitalo, Mr. Mohammad Albooyeh, Dr. Olli Luukkonen, Mr. Younes Radi, Mr. Mohammad Sajjad Mirmoosa, Mr. Victor Asadchy, Mr. Mikhail Omelyanovich, Mr. Joni Vehmas, Dr. Vladimir Podlozny and Dr. Antti Karilainen. Our discussions in the Friday seminars were very helpful and memorable.

I am very grateful to Dr. Stanislav Maslovski, Dr. Alexander Sochava and Prof. Andrei Cherepanov for guiding and advising me in my master's thesis work. This doctoral thesis would have not begun without your teaching and support.

Special thanks go to my co-authors: Dr. Victor Ovchinnikov, Mr. Mikhail Omelyanovich, Dr. Aleksi Tamminen, Mrs. Maria Morits, and Prof. Sergei Tretyakov. Your help and contribution was invaluable.

It is my pleasure to thank the former director of Graduate School in Electronics, Telecommunications and Automation, GETA, Prof. Ari Sihvola and former GETA coordinator Mrs. Marja Leppäharju. GETA not only financially supported the author, but also provided high-quality doctoral courses and organized unforgettable and inspirational seminars.

I want to thank my friends and colleagues, Vasili, Mikhail, Irina, Evgeny, Elena, Daria, Mohammad, Younes, Tomás, Tero, Antti, Pekka, and Olli, just

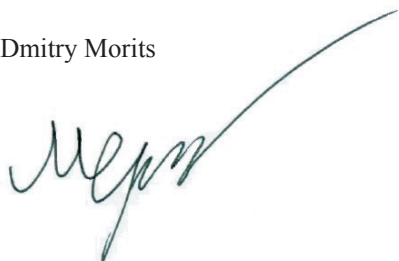
to name a few. Thank you for providing relaxing and entertaining company during office hours and otherwise.

Thank you to my parents, Konstantin and Natalia, as well as my parents-in-law, Valentin and Elena, for supporting and encouraging me.

Finally, I send my warmest thanks to my dear wife Maria for your love and support. You have not only inspired me these years, but even helped with fabrication of samples for our joint paper. You are the most important part of my life, and I love you with all my heart.

Espoo, March 27th, 2014

Dmitry Morits

A handwritten signature in black ink, appearing to read 'Dmitry Morits', with a long, sweeping flourish extending upwards and to the right.

# Contents

<b>Preface</b> .....	5
<b>Contents</b> .....	7
<b>List of publications</b> .....	8
<b>Author’s contribution</b> .....	9
<b>List of abbreviations</b> .....	11
<b>List of symbols</b> .....	12
<b>1. Introduction</b> .....	15
<b>2. Artificial magnetism and negative refraction in the optical range</b> 19	
2.1 Concept of plasmonic nanoring and nanoshell.....	21
2.2 Core-shell spherical clusters.....	28
2.3 Discussion and future research.....	32
<b>3. Electromagnetic characterization of metamaterials</b> .....	34
3.1 Characterization of clustered metasurfaces.....	38
3.2 Dynamic homogenization of bulk MtMs .....	41
3.3 Discussion .....	44
<b>4. Stretchable multifunctional metasurface</b> .....	46
4.1 Design of a multifunctional metasurface.....	47
4.2 Fabrication and measurements .....	50
4.3 Discussion and future research.....	47
<b>5. Conclusions</b> .....	53
<b>6. Summary of publications</b> .....	55
<b>Bibliography</b> .....	57
<b>Publications</b> .....	68



# List of publications

This thesis consists of an overview and of the following publications, which are referred to in the text by their Roman numerals.

- I.** D. K. Morits and C. R. Simovski, “Negative effective permeability at optical frequencies produced by rings of plasmonic dimers”, *Phys. Rev. B*, vol. 81, no. 20, p. 205112 (7 pages), May 2010.
- II.** D. Morits and C. Simovski, “Electromagnetic characterization of planar and bulk metamaterials: A theoretical study”, *Phys. Rev. B*, vol. 82, no. 16, p. 165114 (10 pages), Oct. 2010.
- III.** D. Morits and C. Simovski, “Isotropic negative effective permeability in the visible range produced by clusters of plasmonic triangular nanoprisms”, *Metamaterials*, vol. 5, no. 4, pp. 162-168, Jun. 2011.
- IV.** D. Morits and C. Simovski, “Isotropic negative refractive index at near infrared”, *J. Opt.*, vol. 14, no. 12, p. 125102 (7 pages), Nov. 2012.
- V.** D. Morits, M. Morits, V. Ovchinnikov, M. Omelyanovich, A. Tamminen, S. Tretyakov and C. Simovski, “Multifunctional stretchable metasurface for the THz range”, *J. Opt.*, vol. 16, no. 3, p. 032001 (7 pages), Feb. 2014.

## **Author's contribution**

### **Publication I: “Negative effective permeability at optical frequencies produced by rings of plasmonic dimers”**

The work was mainly done by the author. The author proposed the idea, carried out the design, theory, and simulations, and was responsible for writing the publication. Prof. Constantin Simovski supervised the work.

### **Publication II: “Electromagnetic characterization of planar and bulk metamaterials: A theoretical study”**

The work was mainly done by the author. The idea of the homogenization method was proposed by Prof. Constantin Simovski. The author carried out the design and simulations and was responsible for writing the publication. Prof. Constantin Simovski supervised the work.

### **Publication III: “Isotropic negative effective permeability in the visible range produced by clusters of plasmonic triangular nanoprisms”**

The work was mainly done by the author. The author proposed the idea, carried out the design, theory, and simulations, and was responsible for writing the publication. Prof. Constantin Simovski supervised the work.

#### **Publication IV: “Isotropic negative refractive index at near infrared”**

The work was mainly done by the author. The author proposed the idea, carried out the design, theory, and simulations, and was responsible for writing the publication. Prof. Constantin Simovski supervised the work.

#### **Publication V: “Multifunctional stretchable metasurface for the THz range”**

The work was mainly done by the author. The initial idea was suggested by Prof. Sergei Tretyakov and developed by the author. The author carried out the design, theory, and simulations. Mrs. Maria Morits fabricated the PDMS substrate. Fabrication of the silicon mask and the final film samples was conducted by the author with the help of Mr. Michail Omelyanovich, under the supervision of Dr. Victor Ovchinnikov. The measurements were conducted by the author and Dr. Aleksii Tamminen. The author had the main responsibility for writing the publication. The part of the manuscript concerning fabrication issues was written by Dr. Victor Ovchinnikov. The work was guided by Profs. Constantin Simovski and Sergei Tretyakov.

## List of abbreviations

2D	two-dimensional
3D	three-dimensional
ICP-RIE	inductively coupled plasma reactive-ion etching
MS	metasurface
MtM	metamaterial
NIM	negative-index metamaterial
NRW	Nicolson-Ross-Weir
PDMS	polydimethylsiloxane
TE	transverse electric field
TM	transverse magnetic field

# List of symbols

$a$	radius of sphere [m]
$a_1$	electric dipolar term of series expansion
$b$	lateral size of nanoprism [m]
$b_1$	magnetic dipolar term of series expansion
$C$	capacitance [F]
$D$	size of unit cell [m]
$d$	intersection parameter of dimer [m]
$\mathbf{E}$	electric field strength [V/m]
$f$	distance between adjacent nanorings [m]
$G$	shunt sheet admittance of metasurface
$\mathbf{H}$	magnetic field strength [A/m]
$h$	height of nanoprism [m]
$I$	complex current [A]
$\mathbf{J}$	electric current density [A/m <sup>2</sup> ]
$j$	imaginary unit
$k$	wavenumber [1/m]
$l$	thickness of substrate [m]
$\mathbf{m}$	magnetic dipole moment [Vms]
$N_d$	concentration of clusters [1/m <sup>3</sup> ]
$n$	refractive index
$q$	wavenumber of lattice eigenwave [1/m]
$R$	reflection coefficient
$\mathbf{r}$	position vector [m]
$r_1$	inner radius of core-shell particle [m]
$r_2$	outer radius of core-shell particle [m]
$S$	area of loop [m <sup>2</sup> ]
$s$	interaction constant
$T$	transmission coefficient
$V$	volume of integration [m <sup>3</sup> ]
$X$	series sheet impedance of metasurface

$x$	lattice period [m]
$Z$	impedance [ $\Omega$ ]
$\alpha_{ee}$	electric polarizability [ $\text{m}^3$ ]
$\alpha_{mm}$	magnetic polarizability [ $\text{m}^3$ ]
$\gamma$	auxiliary parameter for wave impedance
$\varepsilon$	relative permittivity
$\varepsilon_0$	vacuum permittivity [As/Vm]
$\lambda$	wavelength [m]
$\mu$	relative permeability
$\mu_0$	vacuum permeability [Vs/Am]
$\chi_{ES}$	electric surface susceptibility [m]
$\chi_{MS}$	magnetic surface susceptibility [m]
$\omega$	angular frequency [rad/s]



# 1. Introduction

Metamaterials (MtMs) are effectively continuous artificial composites, engineered to possess advantageous electromagnetic properties not normally met in nature. Unusual behavior of such composites arises from properties of their individual constituents, which are optically (electrically) small inclusions – particles of ordinary materials like metals and dielectrics. The proper design of MtMs is an optimization of the material, shape and mutual arrangement of inclusions in the host medium. One of the most effective ways of obtaining extreme properties of MtMs is utilization of resonant inclusions, whose electromagnetic response in the given frequency range is very strong in spite of small sizes. The stronger the excitation of constitutive inclusions by the electromagnetic field is, the greater the difference of the MtM from a natural material is.

The design of MtMs starts from the analysis of their constituents. For optically small particles, it implies relations of induced electric and magnetic dipole moments to applied electric and magnetic fields. For MtMs design at this stage, the main challenge is tailoring of resonant dipole responses of inclusions. The physical phenomena behind these resonances can be manifold. In the radio frequency range, the needed resonant behavior can be granted by complex-shaped metal wire particles. This approach allows for the engineering of their electric and/or magnetic response by proper choice of their shape and size. Another microwave example is small spheres, say, of ferrite or of ceramic materials with high refraction index, whose behavior can be described by the well-known Mie theory. Electric and magnetic properties, in this case, are controlled by the fitting of size and material of the spheres. At optical frequencies, the resonant response of optically small inclusions of silver or gold is usually related to the so-called plasmon resonance, strongly affected by the shape and especially by the material properties of metal.



At the same time, electromagnetic composite is not a conglomerate of independent blocks. Mutual interactions between constitutive parts are a very important feature of MtMs and play a huge role in their operation. The most efficient way to describe electromagnetic behavior of a composite is the utilization of averaged material parameters, which in a condensed form sum up properties of individual inclusions and interactions between them. The procedure of introducing such parameters is called homogenization, and for MtM design this is a separate important problem. For bulk composites, the material parameters are effective permittivity and permeability, calculated via volume averaging of microscopic polarization responses or extracted from scattering data for flat layers. In the case of optically thin planar MtMs, also known as metasurfaces or metafilms, volume averaging of the microscopic responses and fields may lose physical meaning. Bulk parameters, such as effective permittivity and permeability, then become inadequate. Instead, metasurfaces can be described by a special type of effective parameters introduced via surface averaging. Whatever method is used for homogenization, the resulting parameters should describe the electromagnetic response of MtM and provide a direct relation between incident and scattered fields, taking into account intrinsic properties of inclusions and interaction between them.

This doctoral thesis is devoted to the study of MtMs consisting of different types of resonant inclusions. The thesis is divided into three research problems, in which resonant electromagnetic behavior plays the key role. The main goals are the engineering of novel and extreme electromagnetic properties in different frequency ranges and the study of MtM homogenization techniques. The methods being used are mainly analytical and semi-analytical modeling, verified by full-wave numerical simulations of Maxwell's equations and experimental measurements, if possible.

The first chapter of the thesis is focused on the extreme material properties in the optical range, arising from the plasmon resonance of silver nanoparticles and Mie resonances of transparent semiconductor particles. It is known that at such high frequencies as near-infrared and visible range, natural materials do not possess magnetic properties; in other words, any

natural material has permeability equal to unity. However, by utilization of properly arranged metal inclusions, one can engineer an artificial magnetic response of the MtM in optics. Previously, it was engineered for MtMs, essentially anisotropic and/or possessing the strong spatial dispersion, which dramatically restricts the applicability of the effective permeability. The goal of the present study is not only to obtain the negative permeability at optical frequencies – the target is to synthesize the isotropic effective continuous material which can be described by a scalar permeability. It is shown that such an ambitious goal is achievable through optimization of the particles' shape and arrangement. In Chapter 2, two design solutions are proposed, one of which allows isotropic negative permeability on the edge between visible and near-infrared ranges. Further, the problem of the negative material parameters in the optical range is developed towards realization of the isotropic negative refractive index. Negative index isotropic MtMs allow such effects as all-angle negative refraction and cloaking; they are often mentioned with respect to so-called super-lensing. Therefore their creation is an important problem for modern metamaterial science, and this part of the work was supported by the FP7 collaborative scientific project METACHEM. Negative refractive index requires both negative permeability and permittivity in the same frequency range, which is obtained by combination of plasmon electric and Mie magnetic resonances in the core-shell spherical particles.

The second research problem investigated in the thesis is an adequate electromagnetic characterization of designed MtMs. The most known and widely utilized method for calculation of material parameters for bulk MtMs is the Maxwell-Garnett technique. This method is simple, but is based on the quasi-static approximation not only for an individual response of an inclusion – it also replaces the electromagnetic interaction between inclusions by their electro- and/or magneto-static interactions. In Chapter 3, one utilizes another approach based on the proper account of electromagnetic interaction between crystal planes forming an orthorhombic lattice of a bulk MtM, whereas these crystal planes are treated as metasurfaces. The applicability of effective surface parameters for

characterization of a metasurface formed by clusters of metal nanoparticles is studied. Then, the dynamic theory, which expresses bulk material parameters of the orthorhombic lattice through surface parameters of constitutive metasurfaces, is applied. This way, the isotropic magnetic MtMs, based on raspberry-like clusters of plasmonic spheres, is homogenized.

The last research problem concerns novel flexible metasurfaces operating in the THz range and based on elastic polymers. Utilization of elastic polymers as substrates for resonant particles allows the stretching, which may strongly affect the operation of MtMs. Such MtMs seem to be promising for sensing applications. In principle, such metasurfaces can be developed for different frequency ranges, from microwaves to optics. It is shown in Chapter 4 that, in the suggested resonant metasurface, the strong sensitivity to stretching can be combined with other interesting electromagnetic properties, such as polarization transformation. This way, a concept of multifunctional stretchable resonant metasurfaces for terahertz frequency range is introduced. The metasurface is studied analytically, numerically, and experimentally. For the creation of experimental samples, an original fabrication process has been developed.

The concluding remarks from the three research problems are presented in Chapter 5, and the summary of Publications describing scientific contributions of this thesis is given in Chapter 6.

## 2. Artificial magnetism and negative refraction in the optical range

Electromagnetic properties of natural materials around us are unbalanced: the electric response in most materials is much stronger than the magnetic one. It is reflected in the fact that non-unitary permittivity is very common, although permeability noticeably differs from unity only for a few narrow classes of materials, namely ferromagnetics, ferrites, and antiferromagnetics. The fundamental reason for this difference is the absence of magnetic charges postulated by the Gauss law for magnetism. The absence of natural magnetic charges, resulting in the absence of natural magnetic currents and conductors, explains the non-parity of electric and magnetic effects. However, it is possible to engineer effective magnetic currents and polarizations created by electric sources and electromagnetic fields. The idea of magnetic polarization originating from circulating electric currents is the main concept of artificial magnetism. The magnetic moment  $\mathbf{m}$  of an arbitrary current distribution in space is described by the following equation:

$$\mathbf{m} = \frac{\mu_0}{2} \int \mathbf{r} \times \mathbf{J} dV \quad (1)$$

where  $\mathbf{r}$  is the position vector pointing from the origin to the location of the volume element, and  $\mathbf{J}$  is the current density vector at that location. Formula (1) shows that a circulating current can be considered as a basic artificial magnetic element – for a closed loop with uniform linear current  $I$  flowing around the area  $S$ , it gives  $m = \mu_0 IS$ , whereas the vector  $\mathbf{m}$  is directed orthogonally to the loop's plane.

The problem of artificial magnetism at high frequencies is one of the most developed chapters in MtM science nowadays. The reason for its importance is a close connection to another major problem, negative refractive index MtMs (NIMs). Already in 1967, Veselago [1] has shown

that it is physically possible to realize such material if one is able to obtain both negative permittivity and permeability in the same frequency range. It was theoretically proved that NIMs allow a remarkable combination of unusual physical phenomena - backward wave propagation, all-angle negative refraction, negative radiation pressure, and reversed Cherenkov radiation. It is important that the possibility of backward wave propagation and negative refraction for the first time was claimed for an isotropic media. In 2000, Pendry, in his seminal work [2], showed that a slab of ideal NIM can work as a so-called super-lens, restoring an exact (point-like) image of a point source at two points, one of them (an inverted image) located at the rear side of the slab. For the microwave realization of NIM, one proposed two main concepts. The first approach was based on the network of intersecting transmission lines supporting backward waves, see [3]. This network operated as a planar analogue of a bulk NIM. The second one is utilization of so-called double split-ring resonators [4] for creating the resonant artificial magnetism allowing the negative  $\mu$ . A uniaxial version of a bulk NIM was then realized by embedding regular arrays of split-ring resonators alternating with parallel wires into a host medium. The development of this approach included design solutions for split rings at higher frequencies, from terahertz to near infrared range [see e.g. 5-9]. An intrinsic property of split-ring resonators is the ultimate anisotropy of their magnetic properties due to their geometry, which makes it challenging to engineer an isotropic magnetic scatterer, keeping it sufficiently small compared to the wavelength. The realization of an isotropic unit cell with split-rings was first suggested in [10] and later (with a more proper orientation of ring gaps) in [11], theoretically allowing the isotropic negative permeability in the microwave range. However, straightforward scaling of split rings for obtaining the negative permeability at optical frequencies turned out not to be very fruitful: in this size scaling, the magnetic resonance saturates due to the high kinetic inductance of metal at optical frequencies that, together with high Ohmic losses of metallic features, does not allow for the achievement of the negative permeability, even in the near-infrared range (and moreover in the visible) [12]. The same reason hinders the implementation of backward-wave transmission lines

networks at optical frequencies. These factors urged researchers to look for other design solutions in order to achieve the negative magnetism in the visible and near-infrared ranges. The most popular design solution allowing the negative permeability in these ranges is the so-called optical fishnet – a bilayer of regularly hollowed plasmonic nanofilms separated by a dielectric nanogap (see e.g [13-15]). However, optical fishnets possess an intrinsically ultimate anisotropy. Our target is isotropic negative magnetism in the visible or near-infrared ranges.

## **2.1 Concept of plasmonic nanoring and nanoshell**

One of the most promising designs for the negative magnetism in optics is the so-called plasmonic nanoring proposed by A. Alù, A. Salandrino and N. Engheta in [16]. This nanoring is an analogue of a spring ring resonator, where the silver or gold nanospheres substitute planar metal features, and the gaps between the adjacent spheres play the role of capacitive loads. The replacement of a solid metal strip by a few distanced spheres allows the suppression of the overall kinetic inductance of such the loop cluster. If a nanoring formed by metal spheres is excited by an alternating magnetic field oriented orthogonally to the ring's plane, the induced electric dipole moments of the spheres are azimuthally circulating around the vector of the magnetic field. This effective circulating current, originating from the electric polarization of nanospheres, produces the magnetic moment, which is resonant due to the plasmon resonance of nanospheres. The magnetic resonance frequency and amplitude is mainly determined by the plasmon resonance of single inclusions, unlike classical split-rings, where the size of the loop is the main parameter.

Later, this idea was developed in [17] in order to achieve the isotropy of the magnetic response of the cluster. The main idea of [17] is as follows. Optically small metal spheres are arranged on a bigger dielectric core in a spherical pattern to form an effective nanoshell, still sufficiently small

compared to the wavelength. This nanoshell can be considered as a spherical shell of resonant dielectric metamaterial and represents the 3D analogue of such a 2D object as a plasmonic nanoring [16]. The response of the nanoshell is determined by that of its constituents – plasmonic metal nanospheres. Since these spheres are very small, it is definitely the dipole response. The ratio of the electric dipole moment of any scatterer to the local electric field produced by all external sources at the scatterer’s center is called the electric polarizability of the scatterer (notice, that the magnetic polarizability is defined as the ratio of the magnetic moment to the local magnetic field). For a single sphere, the electric polarizability is given by the following equation:

$$\alpha_{ee} = \left[ \left( 4\pi a^3 \varepsilon_h \frac{\varepsilon - \varepsilon_h}{\varepsilon + 2\varepsilon_h} \right)^{-1} + j \frac{k_h^3}{6\pi \varepsilon_h} \right]^{-1}, \quad (2)$$

there  $a$  is the sphere radius,  $\varepsilon$  is material (metal) complex permittivity,  $\varepsilon_h$  is permittivity of host medium and  $k_h$  is wavenumber in the host medium. Here and throughout the manuscript, the time dependence is assumed to be  $e^{j\omega t}$ . The real part of permittivity of metals at optical frequencies is negative, and the imaginary part of  $\varepsilon$  for gold and silver is rather small. This allows very strong excitation of a gold or silver nanosphere around a frequency, where  $\varepsilon = -2\varepsilon_h$ . This effect is known as localized surface plasmon resonance.

In the presence of an external magnetic field, the spherical nanoshell is

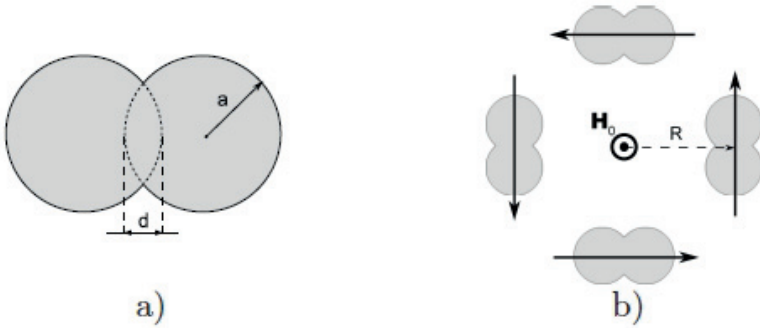


Fig. 1 (a) – A plasmonic dimer with spheres of radii  $a$  and intersection parameter  $d$ . (b) – The effective ring made of plasmonic dimers is excited by a high-frequency magnetic field  $\mathbf{H}_0$  directed orthogonally to its plane. The induced electrical dipole moments are shown by black arrows.

polarized azimuthally with respect to this vector. The nanoshell can then also be treated as an array of closely located coaxial nanorings (such a model was also presented in [17]). If metal spheres are uniformly distributed on the surface of the dielectric core, as it was suggested in [17], the structure works as an isotropic magnetic cluster.

It is important to mention that, in principle, a nanoring is not an ideal magnetic scatterer and besides a dipolar mode excites high-order multipolar components. The impact of these multipolar terms depends on the optical size of the ring and number of particles in it. A thorough study of this problem was carried out in work [18], where it was shown that nanorings of three or more particles can be considered as pure magnetic scatterers in the quasi-static limit. For such structures, the contribution of high-order multipoles is negligible for sufficiently small loops and/or a sufficiently high number of particles. It is interesting to find that if a number of particles is equal to two, i.e. for a pair of nanoparticles, the impact of the electric-quadrupole term is always comparable to a magnetic-dipole one and cannot be neglected even in the quasi-static limit.

The initial model of a nanoring of plasmonic spheres, presented in [16], utilized a well-known Drude model of permittivity of silver. Although, in the visible range, the Drude model estimation of the real part of permittivity

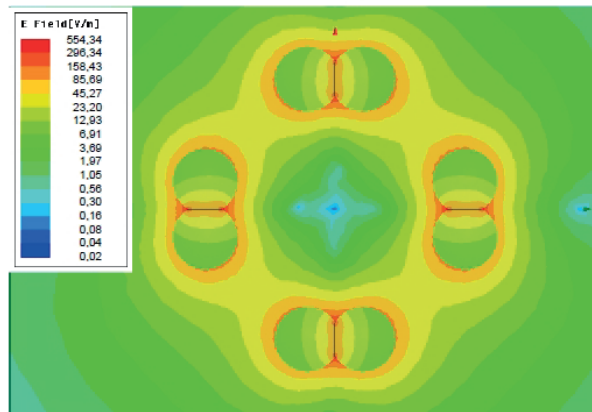


Fig. 2 Spatial distribution of the amplitude of electric field at 369 THz for an effective plasmonic nanoring comprising four dimers with radii  $a = 20$  nm and intersection parameter  $d = 0.3 a$ . Logarithmic scale.



is rather accurate, the imaginary part responsible for losses is seriously underestimated. If, instead of the Drude model, one uses experimental data for the permittivity of silver in the visible range [19], the optimistic results of [17] become invalid. Higher Ohmic losses decrease the magnitude of magnetic resonance, and obtaining the negative permeability with parameters suggested in [17] becomes impossible [1]. In order to overcome the resonance damping by losses, the design of the magnetic nanocluster needs to be more elaborated. One way to modify the design is the utilization of more efficiently polarized nanoparticles than simple spheres. The first modification of spheres was suggested in [1] – plasmonic dimers, i.e. pairs of intersecting silver spheres, as shown in Fig.1. The electromagnetic response of dimers has been studied in the literature [20-22], and it has been shown that the frequency of the plasmon resonance of such nanoparticles lies in the near-infrared range. Replacement of spheres by dimers results in the red shift of the magnetic resonance and the figure of merit, i.e. the relation between the real and imaginary part of the complex permittivity of silver becomes higher. It allows stronger robustness of the resonant properties of a cluster to Ohmic losses, which is crucial for obtaining the negative permeability.

The second important factor is the higher magnitude of plasmonic resonance of dimers due to optimized geometry compared to simple spheres, leading to the increase of total magnetic susceptibility of the effective nanoring. Fig.2 shows the electric field distribution in a nanoring of plasmonic dimers at the frequency of magnetic resonance. The dimers in this simulation are excited by the set of four plane waves providing zero of the electric field and maximum of the magnetic field at the center of the effective ring. Plasmonic resonance behavior is manifested by the strong field enhancement in the vicinity of the dimers, especially in the crevices. At the same time, field distribution clearly demonstrates the concept of an effective circular current arising from individual electric polarizations of plasmonic particles.

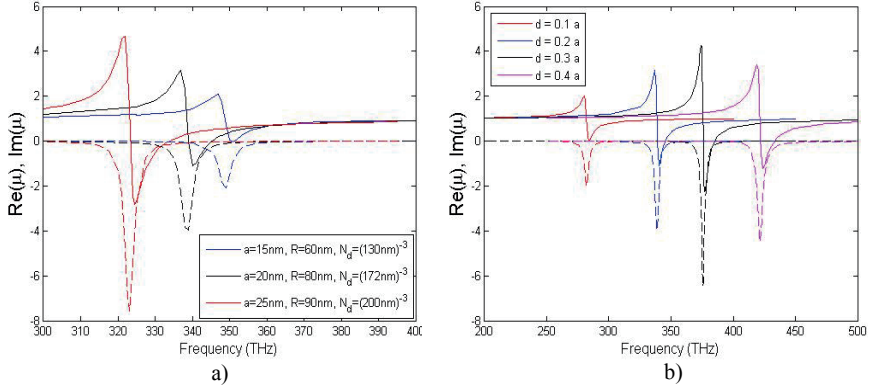


Fig 3 (a) Effective permeability of the composite media made of rings of plasmonic dimers with  $d/a = 0.2$  for different radii of spheres. (b) Effective permeability of the composite media made of effective rings of 4 plasmonic dimers with  $a = 20$  nm,  $R = 80$  nm,  $N_d = (172 \text{ nm})^{-3}$  for different values of parameter  $d$ . Real and imaginary parts of permeability are shown by solid and dashed lines respectively.

The magnetic polarizability of the nanoring can be calculated using a single-dipole approximation model. Each particle is considered as an electric dipole with certain polarizability, allowing calculation of the field scattered by the ring and the total effective polarizabilities, for details see [1]. The calculation of the polarizabilities is followed by the homogenization procedure, in which properties of individual inclusions are taken into account, together with the interactions between them. In [1], to obtain the effective permeability of the composite, the Maxwell-Garnett theory was used. It needs to be noted that this procedure is a quasi-static mixing rule and does not take into account electromagnetic interactions between constitutive components of the composite. The detailed discussion on the alternative methods of homogenization is given in Chapter 3.

Figure 3 shows the effective permeability for different values of spheres radii, intersection, and concentrations of nanorings. One may see that there is an optimal value of intersection parameter  $d = 0.3a$ , for which the resonance of permeability is maximized. For smaller values of  $d$ , the resonance is red-shifted, leading to the decreasing of the optical thickness of the nanoring and hence to weaker resonant properties. For larger values of  $d$ , the resonance shifts into the visible range where the harmful influence of Ohmic losses lead to the resonance damping. The dependence of the

magnetic properties on the spheres radii is more transparent: larger particles possess stronger electric dipolar resonance that leads to the higher magnetic susceptibility of the nanoring. At the same time as increasing the size of particles, one should remember the limitations of the homogenization model, which requires the size of a unit cell  $D$  to be much smaller than the wavelength. For the dimensions shown in Fig. 3 at the resonant frequency  $D \approx \lambda/5 \approx \lambda_{eff}/3$ , where  $\lambda_{eff}$  is a wavelength in the host medium with  $\epsilon_h = 2.2$ . For such optically substantial particles, the quasi-static homogenization model gives only a qualitative estimation of material parameters. This question is further elaborated and more reliable predictions are made.

Utilization of plasmonic dimers allows the negative permeability at the bound between the near-infrared and visible frequency ranges. However, dimers have an important drawback: their geometry is not isotropic, which hinders isotropic magnetism. In order to make a response from a magnetic cluster isotropic, one needs to use other particles, whose plasmon resonance at the same time should be stronger compared to spheres. The design solution was suggested in [III] – it is a cluster of plasmonic triangular nanoprisms, shown in Fig.4. Being uniformly distributed on the top of a dielectric core, nanoprisms form an almost isotropic scatterer.

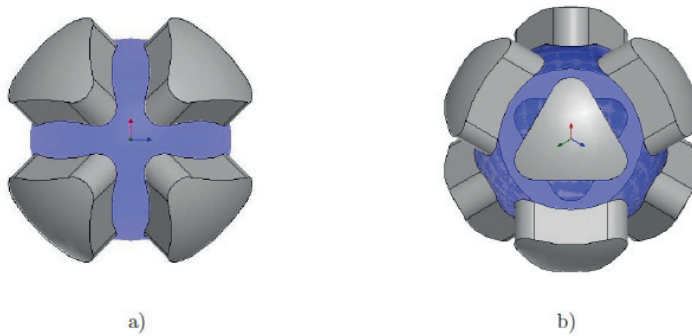


Fig. 4 Cluster made of eight triangular nanoprisms on a dielectric core (two points of view).

Triangular nanoprisms have been studied in the literature previously in works [23-25], and it has been shown that their electric dipole resonance is stronger compared to simple spheres and lies in the low and middle parts of the visible range, depending on lateral size  $b$  and the height of particles  $h$ . In [III], magnetic susceptibility of the cluster was calculated using two methods, showing good agreement with each other. The first one, extraction of polarizabilities of single clusters from reflection and transmission coefficients of a metasurface, is discussed in detail in Chapter 3. The second method is a direct calculation of a magnetic moment using equation (1), where the polarization current density  $\mathbf{J}$  is taken from the full-wave numerical simulations (with standing waves emulating the magnetic excitation of the cluster). The simulations were performed using Ansoft HFSS commercial software. The results show the following dependence on the magnetic polarizability on the particle geometry. On one hand, the increase of  $h$  and  $b$ , i.e. the size of nanoprisms, leads to the strengthening of the magnetic resonance due to a stronger plasmonic response of single inclusions. On the other hand, for larger particles, the resonant frequency is red-shifted, which leads to the decrease in the optical size of the cluster. The

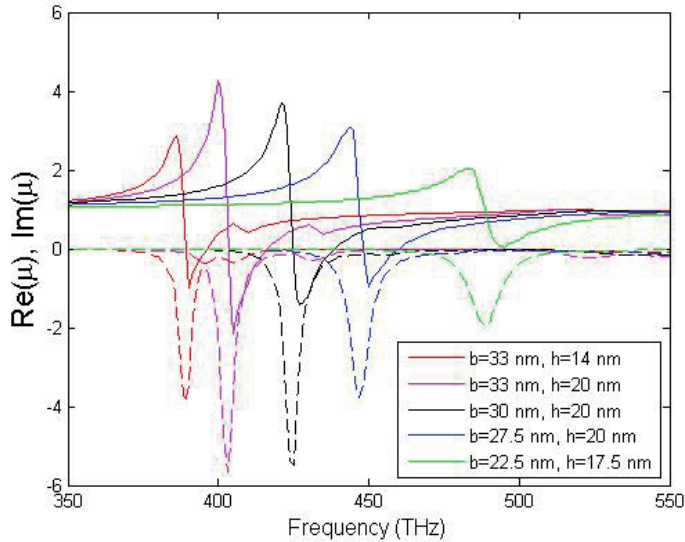


Fig. 5 Effective permeability of the composite made of clusters of triangular nanoprisms with different edge lengths and heights, concentration of clusters in the composite  $N_d = (110 \text{ nm})^{-3}$ . Real and imaginary parts are shown by solid and dashed lines respectively.

smaller optical size leads to the suppression of the magnetic resonance at the lower frequencies. Hence, due to two opposite factors, there are optimal values of  $b$  and  $h$  for the maximum magnetic resonance, which are turned to be  $h = 20$  nm,  $b = 33$  nm. For nanoprisms of this size and concentration of clusters  $N_d = (110 \text{ nm})^{-3}$  the size of the unit cell is about  $D \approx \lambda_{eff}/5$  at the frequency of the magnetic resonance. This is an important improvement compared to the dimer nanoring and gives stronger grounds for utilization of the quasi-static Maxwell-Garnett homogenization procedure. Fig. 5 shows that for the optimal geometry negative permeability is achieved in the red part of the visible range. It is important to mention that the experimental data for the permittivity of silver was taken into account [19]. It means that the design solution provides enough robustness to the Ohmic losses. This robustness is crucial for the artificial magnetism based on plasmonic inclusions.

## 2.2 Core-shell spherical clusters

Utilization of triangular nanoprisms theoretically allows isotropic negative permittivity in the visible range, but our second target – isotropic negative refraction index - is not possible with this design. To obtain an isotropic NIM, one needs to have both negative permeability and permittivity in the same frequency range. In MtM consisting of spherical clusters of plasmonic nanoprisms, or those of simple plasmonic spheres, or plasmonic dimers, the electric and magnetic resonances are separated over the frequency axis. It is possible to make them overlapping, but only by bringing additional losses, which kills the effect of NIM. The solution for this problem is the creation of MtM, in which generic inclusions comprise two parts, each possessing resonant properties: one responsible for the electric resonance and the second one responsible for the magnetic resonance. The main advantage of this approach is that for such complex inclusions, the electric and magnetic resonances can be engineered separately, which allows, by proper fitting of

particle geometry tuning, both resonances into the same frequency range. For these purposes, the magnetic Mie resonance can be utilized, which is a characteristic effect for high-permittivity spheres [26]. At microwaves, this idea was studied in [27]; there, the suggested structure consisted of two sublattices: one of small dielectric spheres for electric resonance and another of big dielectric spheres for magnetic Mie resonance. However, as it was shown in works [28, 29], such composites demonstrate an extreme anisotropy of both refractive index and wave impedance, very heavily depending on the propagation direction (pass-band for one direction is, over the frequency axis, the stop-band for another direction). This extreme anisotropy results from the spatial dispersion. To avoid the spatial dispersion, one needs to somehow unify the sublattices. This is possible via replacing a pair of spheres by a core-shell particle. The first attempt to create such an MtM was given in [30], where the composite was formed by high-permittivity dielectric spheres covered with metallic shells. Metallic nanoshells of constitutive particles provided negative permittivity of the lattice due to their plasmon resonance, whereas the dielectric cores provided negative permeability. With the proper tailoring of particle sizes, the design solution allowed negative refraction in the far infrared; however, it cannot be scaled up to the near-infrared range due to the lack of material with high enough permittivity. This high permittivity is required because the core-shell particles must be well separated from one another. Otherwise, the adjacent metal shells will be capacitively coupled and the design idea will not work. Strong separation, together with the requirement of the optical smallness for a unit cell, imposes non-realistic requirements to the permittivity of the dielectric core.

In [IV], we suggested an alternative design solution also based on core-shell spherical particles. The electric resonance is provided by a metal sphere forming a core of inclusion. The magnetic Mie resonance is exhibited by a silicon dielectric shell (we studied both crystal and amorphous silicon cases). Thus, the resulting inclusion is a core-shell sphere in which a core is made of silver and the shell is made of silicon, crystalline, or amorphous, with relative permittivity of about 12-25 in the visible range

allowing for a strong magnetic response. Metal cores of two closely located particles are separated by optically dielectric (semiconductor) shells, and their capacitive coupling is negligible.

The electric and magnetic polarizabilities of such core-shell particles can be calculated analytically by the generalized Mie theory developed in works [31, 32]. First, the scattered field of the particle is expanded into multipole terms expressed by the combination of spherical functions, for details see [IV]. Then, for optically small particles, high-order terms can be neglected, and only electric and magnetic dipole contributions are taken into account,  $a_1$  and  $b_1$  respectively. Polarizabilities are then calculated using the following expressions:

$$\alpha_{ee} = -\frac{6\pi j a_1}{k_h^3}, \quad \alpha_{mm} = -\frac{6\pi j b_1}{k_h^3}. \quad (3)$$

Utilization of analytical theory allows fast optimization of the particles' size in order to obtain a strong electric and magnetic response in the same frequency range. For a particle made of a silver core and a silicon shell, the optimal inner radius is  $r_1 = 30$  nm and outer radius  $r_2 = 130$  nm, giving the resonant response in the frequency range of about 300-350 THz. At the resonant frequency, the optical size of the particle is about  $\lambda/4$ .

The effective permittivity and permeability are calculated using the

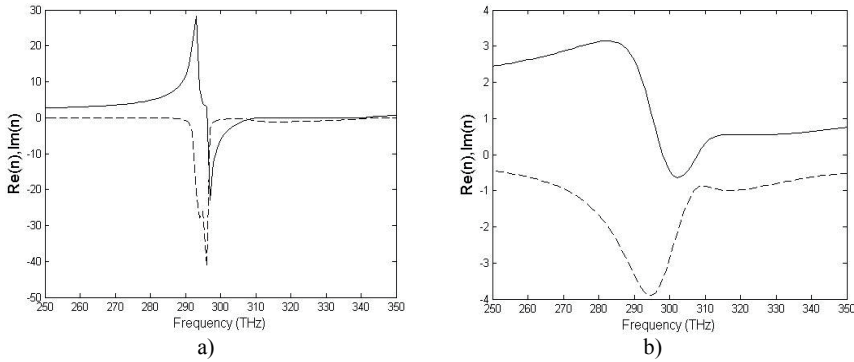


Fig. 6 Dependence of the effective refractive index on wavelength for a three-dimensional array of coated spheres with  $r_1 = 30$  nm,  $r_2 = 130$  nm and unit cell size 270 nm: (a) - for the periodic array with compensated radiation losses; (b) - for the random array. Real and imaginary parts are shown by solid and dashed lines respectively.

Maxwell-Garnett formulas. In [IV], the analytically calculated refractive index is verified by the full-wave simulations of the refraction by an MtM prism (wedge). Since the scattering by the edge is a critical parasitic factor masking the refraction of the incident wave by the wedge in this simulation, a Gaussian beam was used instead of the incident plane wave. The wedge, though composed of core-shell spherical particles with internal regularity, is not infinite. Only in infinite regular arrays of arbitrary particles, their scattering losses (for electric dipoles described by the imaginary term in formula (2), for magnetic dipoles a similar formula exists) are fully suppressed by the electromagnetic interaction of particles (see e.g. in [33]). Therefore, the problem arises: how complete is the compensation of scattering losses in such a realistic MtM sample? This problem, for the present case, is very important, since the plasmon resonance of the metal core in the silicon environment holds in the near infrared range, where the silver has a high figure of merit and where optical losses of silicon are very low. In this case, scattering losses can be comparable to Ohmic losses and even higher. Figure 6 shows an analytically calculated refractive index for an array of core-shell particles for two cases: totally compensated and fully uncompensated scattering losses. In both situations, refractive index reaches negative values, although the amplitude of the resonance differs drastically. The full-wave simulations have shown that the situation is nearly in the middle between these two limit approximations.

Simulations of a Gaussian beam incidence on the prism of core-shell particles showed the following differences compared to the quasi-static analytical model. First, the outer radius of particles in the optimal design is changed from 130 nm to 140 nm. The reason for this effect is dynamic interactions between adjacent shells, not taken into account by Maxwell-Garnett formulas. Dynamic interactions (see the next chapter) lead to the shift of the frequency of magnetic resonance. This effect required an additional optimization of the particle sizes in the vicinity of values predicted by the analytical model. The resulting frequency of the negative refraction is 15% blue-shifted compared to the predictions of the analytical theory. The deviation angle of the beam and its attenuation in the prism give



an estimated refractive index  $n=-0.5-j0.12$ , meaning the essential impact of the scattering losses are only half-compensated by the electromagnetic interaction of particles.

The design solution presented in [IV] was independently suggested in paper [34] and the results of both works are in good agreement with each other. Moreover, the authors of [35] later developed their work and theoretically demonstrated negative refraction by the array of hybrid metal-semiconductor nanowires, which are two-dimensional analogues of the core-shell spheres, perhaps not so challenging for nanofabrication.

### **2.3 Discussion and future research**

Several design solutions presented in this section lead to the artificial magnetism in the optical range, resulting in negative permeability in near-infrared frequencies [I], isotropic negative permeability in the visible range [III], and, finally, in isotropic refractive index in the near-infrared range [IV]. Estimations of the design parameters and of the resulting material parameters of our MtMs in these works were performed theoretically, mainly using the quasi-static model verified and corrected by full-wave simulations. Suggested concepts require verification by the experiment or at least by a more precious theoretical model of homogenization, taking into account dynamic interactions between resonant inclusions. Obviously, the experimental measurements should be preceded by nanofabrication, which is a separate complicated problem for such complex MtMs. Recently, the concept of artificial magnetism for our nanoshells of plasmonic spheres was experimentally proved in [36], where the clusters were fabricated by chemical self-assembly in a liquid solution. The method of fabrication of clusters of triangular nanoprisms was suggested in [37]; however, the preliminary studies have not revealed magnetic response in the optical range, because the fabricators could not avoid a substantial amount of free metal nanoprisms in the gaps between adjacent clusters. Our core-shell

structures seem to be very promising for the experimental realization of optical negative refraction. Core-shell spheres and especially core-shell cylinders, with amorphous silicon shells are, in principle, feasible with modern techniques (see e.g. in [38-41]). However, we have not managed to find the opportunity of their fabrication and cannot present experimental results in this chapter. Concerning further development of homogenization methods for more advanced MtM characterization, theoretical studies presented in the next section can be applied to the suggested MtMs for better estimation of the impact of dynamic interactions in them.

### 3. Electromagnetic characterization of metamaterials

Homogenization is the introduction of material parameters adequately describing, in a condensed form, electromagnetic properties of optically dense arrays of particles. A universe of various homogenization methods developed in the literature can be divided into two main classes: theoretical homogenization and heuristic homogenization (in accord to the terminology suggested in [42]). The first approach starts from the averaging of the microscopic fields and polarizations, resulting in theoretical material equations along with relations between polarizabilities of individual inclusions and collective susceptibilities of the array to the averaged fields, in other words, in effective material parameters of the composite. There are plenty of different approaches for theoretical homogenization. The so-called mixing rules are known from the beginning of twentieth century [43] and are still widely used in the literature for MtM homogenization. In these methods, the interaction between particles is assumed to be a static, fully neglecting dynamic wave process. Among mixing rules, the Bruggeman [44] and Maxwell-Garnett formulas [43] are the most well-known. Due to increasing interest in the MtM field, more elaborated homogenization methods have been developed in the past few years. Several theoretical methods suggested in [45-49] are based on introducing material parameters from the solution of the eigenwave problem for unbounded lattices. Among the recently developed, the method introduced by M. Silverinha [50-52] should be mentioned, in which non-local permittivity and permeability are found from the numerical simulations of fields in unbounded lattices in such a way that all cases of weak spatial dispersion are covered. These parameters, depending on the wave vector, can be used for solving some boundary problems when complemented by so-called additional boundary conditions. The problems that are solvable in this way are those of the plane-wave incidence to parallel-plate MtM layers. The applicability only for layers and plane waves is the main restriction of this homogenization.

The main advantage of this method is that it allows one to take into account excitations of surface polaritons. However, even for these best-known theoretical homogenization techniques, the main problem remains: it is too difficult to utilize for experimental characterization of MtMs. This is the reason why, in the modern literature, heuristic homogenization prevails, in which an MtM sample is assumed to be uniform magneto-dielectric material, and the material parameters are extracted from the scattering data. For slabs illuminated by a normally incident plane wave, the scattering matrix comprises two parameters – reflection ( $R$ ) and transmission ( $T$ ) coefficients. The most popular method is the so-called Nicolson-Ross-Weir (NRW) algorithm, developed originally for natural weakly dispersive magneto-dielectric materials and later applied to MtMs in spite of their resonant dispersion and imperfect optical homogeneity [53-55]. In the NRW method, a slab of MtM is assumed to possess the same scattering characteristics as a slab of equivalent fully homogenous media. Using this assumption, one can apply the inverse Fresnel-Airy formulas, which allow calculation of the effective refractive index  $n_{eff}$  and impedance  $Z_{eff}$  from the  $R$  and  $T$  coefficients of a MtM slab, obtained from the experiment or from full-wave numerical simulations. The effective permittivity and permeability are then calculated by the following expressions:

$$\varepsilon = \frac{n_{eff}Z_0}{Z_{eff}}, \quad \mu = \frac{n_{eff}Z_{eff}}{Z_0}, \quad (4)$$

where  $Z_0$  is an impedance of surrounding media. Due to its simplicity, the NRW method became very popular for the electromagnetic characterization of all new materials (for fully homogeneous materials without spatial dispersion, for MtMs which are homogeneous only conditionally because they obviously possess non-negligible spatial dispersion, and even for discrete materials - photonic crystals). Definitely, for materials which possess even weak spatial dispersion, the application of this simplistic model led to some controversial results and met certain unexpected problems, from which the so-called “antiresonance” effect is, perhaps, the most notable. Reported in numerous works (see e.g. [56-65]), “antiresonant” results of the NRW characterization contained an incorrect sign of the

imaginary part of permittivity or permeability, meaning violation of the passivity condition, and the decay of the real part of permittivity or permeability versus frequency beyond the band of resonant losses, meaning violation of the causality [66,67]. The reasons for such behavior were clarified in some recent works, e.g. in [68]. First of all, a considerable part of MtMs, in principle, cannot be homogenized in terms of effective  $\epsilon$  and  $\mu$  and application of the NRW method for their characterization is meaningless. It refers to planar metamaterials called metasurfaces (or metafilms). Metasurfaces (MSs) are monolayers of resonant scatterers located on a substrate or incorporated into a dielectric matrix. Effective bulk metamaterial that usually models such an array in the dominating literature implies the refracted wave inside it. However, the original monolayer cannot refract the wave. Moreover, the effective thickness of this effective material is a physically meaningless parameter. Fitting this bulk-medium model to exact simulations of  $R$  and  $T$  of an MS may give the thickness smaller than the physical thickness of original particles or larger than the period of their array (see [69-74] for example). Also, the NRW method is often applied for bulk MtMs at high frequencies, where regular MtMs behave as photonic crystals. However, such phenomena of strong spatial dispersion as the Bragg phenomena, Bloch modes, high-order bandgaps, and pass-bands cannot be described via  $\epsilon$  and  $\mu$ . For both MSs and photonic crystals, the NRW method usually results in weird frequency dispersion of retrieved “effective material parameters”.

For bulk MtMs operating in the range where they are optically dense and represent media with only weak spatial dispersion, the failure of the NRW method is usually exhibited in the “antiresonance”, which may be for two reasons [75]. One reason, first pointed out by A. Alù in 2011 [76], is the non-negligible phase shift of the wave per unit cell of the resonant lattice, which is the reason of the impact of the wave interaction of crystal planes through which the lattice eigenwave propagates. This is nothing but weak spatial dispersion in the unbounded lattice. Another reason, pointed out by C. Simovski and S. Tretyakov in 2007 in [77], refers to the finite-thickness layers of MtM. It is an incorrect equation of the retrieved surface impedance to the effective-medium impedance, entering formulas (4). Impedance  $Z_w =$

$\sqrt{\mu/\varepsilon}$  is a wave impedance of the effective medium, expressed through the bulk material parameters, which are, in classical theory, introduced by volume averaging of the microscopic fields over the material unit cell, whereas impedance entering Fresnel equations used in the retrieval procedure is a surface impedance of the same effective medium obtained from the integration over the input or output face of the unit cell. It is shown in [78] that these two impedances are not equal, and the difference between them is of the order of  $(qx)$ , where  $q$  is the wave number of the lattice eigenwave and  $x$  is a lattice period. For natural materials  $qx < 0.01$ , the difference is negligible. Therefore, the NRW procedure perfectly works for natural magneto-dielectrics. However, MtM, as a rule, operates at frequencies so that  $0.1 < qx < 1$ , and the surface impedance of the MtM half-space noticeably differs from its wave impedance. This error produces the “antiresonance” for one of two material parameters when this impedance is combined with the refraction index in formulas (4). This effect, as well as the internal non-locality pointed out by Alù, also results from non-negligible phase shift per unit cell, i.e. also refers to the phenomena of weak spatial dispersion, which makes the direct application of NRW retrieval incorrect for MtMs.

In works [I, III, IV], the Maxwell-Garnett homogenization was mainly utilized for analytical modeling of our MtMs. In order to take into account dynamic interactions between MtM inclusions in [III], another homogenization method was introduced. Its idea is electromagnetic characterization of an orthorhombic lattice as a set of metasurfaces through which the lattice eigenwave propagates. Here, the metasurface (MS) is a homogenized crystal plane – a sheet of electric and magnetic surface polarization. First, the material parameters of constituent MSs are extracted from scattering data, and then the material parameters of bulk MtM are calculated, taking into account dynamic interactions of sheets of electric and magnetic currents. Utilization of the scattering data, together with this dynamic theory, combines the advantages of analytical modelling and full-wave simulations. The first step of the procedure is closely connected with a theory of surface susceptibilities of metasurfaces developed in groups of C.

### 3.1 Characterization of clustered metasurfaces

In works [79, 80], Holloway and Kuester, with coauthors, considered optically dense planar arrays of resonant particles, which were named MSs. It was shown that for such arrays, special material parameters can be introduced called electric  $\chi_{ES}$  and magnetic  $\chi_{MS}$  surface susceptibilities, defined through the jumps of averaged electric and magnetic fields across the MS. For the oblique wave incidence, both tangential and normal components of these fields are involved and both of them have these jumps; so, these susceptibilities are tensor parameters. However, in absence of the bianisotropy, these tensor parameters are split onto scalar values different for TE and TM polarizations. So, non-bianisotropic MSs are described by four surface material parameters. Once extracted from reflection  $R$  and transmission  $T$  coefficients for two arbitrary angles (retrieval formulas are presented in [79, 80]), these parameters allow us to predict  $R$  and  $T$  for any other angle of incidence. For square grids of dipole particles, these surface susceptibilities are directly connected with individual polarizabilities of particles and can be expressed from them by formulas:

$$\alpha_{ee} = \left( \frac{1}{\chi_{ES}x^2} + \frac{1}{4sx^3} + \frac{jk^3}{6\pi} \right)^{-1}, \quad (5)$$

$$\alpha_{mm} = \left( \frac{1}{\chi_{MS}x^2} + \frac{1}{4sx^3} + \frac{jk^3}{6\pi} \right)^{-1}, \quad (6)$$

where  $x$  is a grid period, and  $s$  is an interaction constant of a planar dipole grid (for the detailed explanation of the interaction constant see [32]). The authors of [79, 80] numerically and experimentally verified their homogenization method for the arrays of solid electric and magnetic scatterers in the microwave range. In the homogenization method presented in [II], extraction of surface susceptibilities is suggested as a first step of the algorithm for the characterization of bulk composites made of complex

inclusions – clusters of solid resonant particles. In order to verify the applicability of this method (further referred as the Holloway-Kuester method) for clustered structures in works [I,III,IV], surface susceptibilities of MSs formed by magnetic nanoclusters were extracted from  $R$  and  $T$ , obtained by full-wave numerical simulations, then electric and magnetic polarizabilities of an individual cluster were calculated using Eqs. (5-6) and compared to those obtained by different methods. First, MS made of Alù-

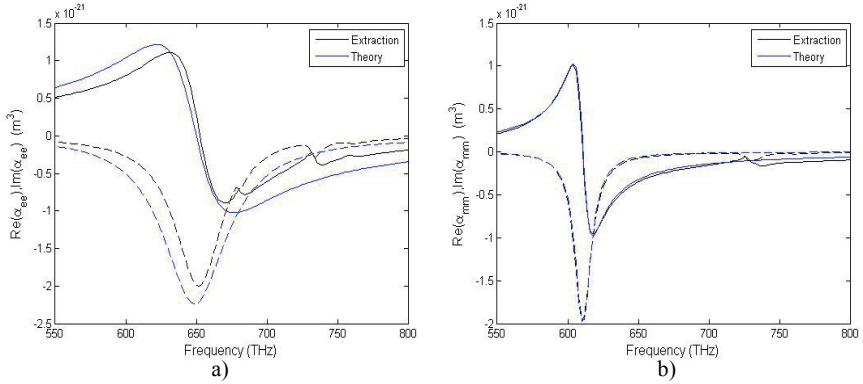


Fig.7 (a) Electric and (b) Magnetic polarizability of an effective ring of four plasmonic spheres with  $a = 16$  nm,  $R = 38$  nm. Black curve - extracted from the reflection and transmission coefficients of an individual grid; blue curve – calculated using the single-dipole theory. Real and imaginary parts are shown by solid and dashed lines respectively.

Salandrino-Enggheta nanorings of plasmonic spheres, embedded into uniform  $\varepsilon = 2.2$  media was studied with radii of spheres  $a = 16$  nm, radius of nanorings  $R = 38$  nm, and distance between the closest edges of two adjacent nanorings  $f = 9$  nm. The comparison of effective polarizabilities of a nanoring calculated using Eqs. (5-6) (and full-wave simulations for two incidence angles from which the surface susceptibilities were retrieved) with those obtained from the single-dipole model of nanospheres [16] is shown in Fig.7. Surprisingly, the plots show good agreement, despite the fact that the size of the unit cell is as substantial as  $\lambda_{eff}/3$  at the resonant wavelength. To confirm that the retrieved susceptibilities are really material parameters of our MS in work [II], the  $R$  and  $T$  coefficients were analytically calculated for different angles via retrieved surface susceptibilities and then compared to simulated  $R$  and  $T$ . This comparison revealed quite a noticeable difference only in a very narrow band around the resonance frequency, but the overall



prediction of the scattering parameters via the retrieved by the method is rather accurate. In [III], the electric and magnetic polarizabilities of clusters of plasmonic triangular nanoprisms were extracted using the same Holloway-Kuester retrieval method and compared to polarizabilities calculated via numerical integration of polarization currents over the volume of the nanoring (these polarization currents were obtained by full-wave simulations). Results again showed good agreement, surprising for such substantial clusters, providing another argument in favor of surface material parameters for electromagnetic characterization of clustered plasmonic

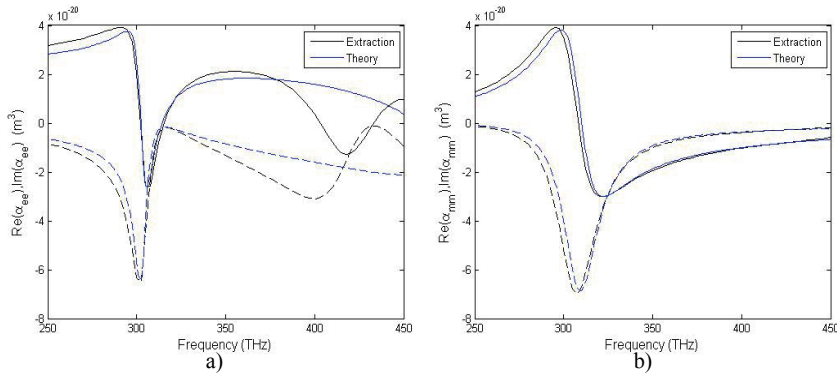


Fig. 8(a) Electric and (b) Magnetic polarizability of silver-silicon core-shell cluster with radii  $r_1 = 30 \text{ nm}$ ,  $r_2 = 130 \text{ nm}$ : blue - calculated by the Mie theory, black – calculated by Holloway-Kuester method. Real and imaginary parts are shown by solid and dashed curves respectively.

MSs.

In [IV], the individual polarizabilities of the core-shell spherical clusters were obtained by the same procedure and compared to analytical results offered by the Mie theory generalized for core-shell spheres. Figure 8 shows the plots for the arrays with a unit cell size of 270 nm. The methods give very good agreement up to frequencies where the optical size of the unit cell exceeds  $\lambda_{eff}/3$  (i.e. it works until  $qx=2$ ). This and the previous examples show that despite the fact that the Holloway-Kuester theory was developed for arrays of simple solid particles and formulas, (5, 6) are clearly quasi-static approximations, it is in fact a powerful tool, suitable for the characterization of MSs of complex-shape and multi-particle constituents and applicable at frequencies twice exceeding the standard bound of the

quasi-static region  $qx=1$ .

### 3.2 Dynamic homogenization of bulk MtMs

The homogenization procedure for bulk MtMs suggested in [II] starts from the extraction of the surface susceptibilities of its constituent MSs from  $R$  and  $T$  coefficients, obtained from numerical simulations or experimentally. It was shown that the susceptibilities are, in fact, equivalent to the shunt sheet admittance  $jG$  and series sheet impedance  $jX$  of an individual MS:

$$G = k\chi_{ES}, X = -k\chi_{MS} \quad (7)$$

These parameters were derived in [68], in the theoretical electrodynamic model of grids of electric and magnetic dipoles, called  $p$ - $m$  lattices. In [68], it was shown that, for orthorhombic arrays of  $p$ - $m$  dipoles, one can derive the following dispersion equation:

$$\cos qx = \cos kx - (1 + \sqrt{1 - \Phi}) \left( \frac{G + X}{4} \right) \sin kx, \quad (8)$$

where it is denoted

$$\Phi = \frac{GX \cos kx}{2(\sin kx)^2} \left( \frac{4+GX/2}{G+X} \cos kx - \sin kx \right). \quad (9)$$

The dispersion equation was derived, neglecting near-field interaction of adjacent crystal planes, i.e. their coupling through high-order Floquet harmonics and under the quasi-static assumption  $qx < 1$ . The agreement between the quasi-static surface susceptibilities retrieved earlier and the sheet admittance and impedance directly calculated using the quasi-static model shows again that the quasi-static model remains valid well beyond its initial limitations.

The idea of the homogenization procedure is utilization of  $G$  and  $X$  (or equivalently  $\chi_{ES}$  and  $\chi_{MS}$ ) obtained from  $R$  and  $T$  of a single grid for solution of the dispersion equation (8). The wave impedance is then found from the following expression:

$$Z_w = Z_0 \frac{\gamma k + q}{\gamma q + k} \quad (10)$$

where  $\gamma$  is an auxiliary parameter found from  $G$  and  $X$ , defined in [II].

Bulk material parameters of the composite are then expressed through the wavenumber and wave impedance:

$$\varepsilon_{dyn} = \frac{q}{\omega Z_w}, \quad \mu_{dyn} = \frac{q Z_w}{\omega} \quad (11)$$

It is important to mention that although equation (11) coincides with the expression used in the NRW method, the impedance entering (4) is now a wave impedance instead of a surface impedance. This correction prevents the anti-resonance artifact inherent to MtMs characterized via the NRW procedure.

In [II], the suggested homogenization method was applied to the nanorings of plasmonic spheres, whose polarizabilities are presented in Fig.7. The effective material parameters are shown in Fig.9.

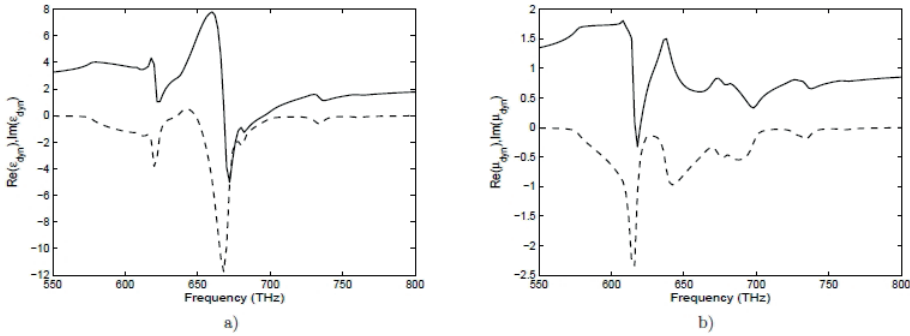


Fig.9 Effective material parameters of the composite media of effective nanorings of silver spheres with parameters  $a = 16$  nm,  $R = 38$  nm,  $x = 96$  nm: (a) – Effective permittivity obtained using the dynamic model. (b) – Effective permeability obtained using the dynamic model. Real and imaginary parts of all parameters are depicted by solid and dashed lines, respectively.

Material parameters obtained by dynamic homogenization in most of the frequency range satisfy passivity and causality, which is a good indicator of the physical adequacy of the applied method. Within the narrow range of 640-650 THz, where  $qx = 2.5$ , the imaginary part of permittivity has the wrong sign, meaning that homogenization fails for this range due to the effective wave shortening. The reason for this artifact is the utilization of

simplifying assumptions in the model, namely neglecting high-order Floquet modes. We believe that taking into account these modes would improve the accuracy and would allow us to get rid of this small artifact. However, such a modification of the theory will lead to a serious complication of the model and will make our theory cumbersome and difficult. At the same time, our results are different from the predictions of the quasi-static (Maxwell Garnett) homogenization model. First of all, electric and magnetic modes are not independent: the permittivity possesses a small resonance at the frequency of the main magnetic resonance and vice versa. This is a logical consequence of our dynamic homogenization, in which  $p$ - $m$  interactions are taken into account (unlike the quasi-static model, in which the electric dipoles do not interact with the magnetic ones). It is important that this  $p$ - $m$  interaction is not bianisotropy, since it is manifested by the complementary resonance of the effective permittivity. However, it is a clear manifestation of weak spatial dispersion, analogous to the bianisotropy. In principle, this interaction can be transposed from the effective permittivity into a new material parameter – magneto-electric coupling coefficient of non-bianisotropic MtMs, as it was suggested by A. Alù in [76] (this approach was further elaborated in [81]). Similarly, this interaction can be removed from the effective permeability, and both effective-medium parameters become Lorentzian. However, in [II], we have not made this transformation since our work was published before [76]. We also avoid this transformation because our complementary resonances resulting from the  $p$ - $m$  interactions are approximately Lorentzian and do not urge us to introduce Alù’s additional material parameter to make the homogenization model more adequate (the “antiresonances” will appear only if we remove losses from our simulations).

First resonance of the permeability at 600-630 THz is complemented with complementary resonance of the permittivity. The main electric resonance holds within the region of 640-680 THz. The second magnetic resonance holds in this region and is complementary. Regarding more high-frequency resonances – the electric and magnetic ones at 740-750 THz refer to strong spatial dispersion – above 730 THz the lattice period exceeds half-wavelength and the homogenization becomes inadequate (as well as it is in

the range 640-650 THz due to the resonant wave shortening).

### 3.3 Discussion

The suggested homogenization procedure, based on the representation of a lattice as a set of MSs, reveals the effects ignored by the quasi-static model. At the same time, the goal of introducing the material parameters is the easy solution of boundary problems. In the quasi-static limit all we need to solve boundary problems is effective material parameters, since macroscopic fields satisfy Maxwell boundary conditions, but beyond this limit it is not so. Indeed, relationships between the macroscopic field and the local field derived by volume averaging for unbounded lattices are not fulfilled at the boundaries, where a part of the integration volume lies in free space air and another part inside the effective medium. The error related to this is negligible only in the quasi-static limit. Application of the Maxwell boundary conditions, together with the material parameters (derived for an unbounded MtM), brings an error of the order  $(qx)$ , which may be crucial for electromagnetic characterization. A possible solution for this problem is the utilization of special transition layers, as it was suggested by C. Simovski in [68], or excessive surface polarization sheets, as it was independently suggested by two scientific groups in works [82, 83]. The approach [68] can be considered as the development of the idea by Drude [84], where one suggested that Maxwell's boundary conditions are not fulfilled for natural crystals and was suggested to compensate their violation introducing the transition layers with thickness equal to the lattice period. The Drude transition layers turned out to be irrelevant for natural lattices, however for MtMs, this idea allowed the self-consistent model of a finite-thickness bulk layer without "antiresonance". However, the set of material parameters of transition layers turned out to be different from those of the bulk material sandwiched between them. The description of transition layers in terms of effective permittivity and permeability is meaningless, and only the refraction index and wave impedance can be introduced. In the second approach [82, 83], the MtM slab is modelled by a homogeneous layer

sandwiched between two infinitesimally thin sheets of surface electric and magnetic polarizations. These fictitious MSs emulate the jumps of tangential components of the macroscopic electric and magnetic fields across the physical boundary of the MtM. This model, where the error of Maxwell's boundary conditions at the interfaces is compensated by excessive fictitious MSs, seems more promising for the retrieval procedure than the model with finite-thickness transition layers [68]. However, if the impact of surface polaritons excited at the surfaces of a finite-thickness MtM lattice is significant, the straightforward retrieval of material parameters becomes impossible. In this case, the homogenization model, based on Silveirinha's non-local effective material parameters and additional boundary conditions, may be fit to be measured or numerically simulated  $R$  and  $T$  coefficients of the MtM slab.

## 4. Stretchable multifunctional metasurface

Tunability and controllability of MtMs are among the most popular topics in modern MtM science. There are plenty of possible solutions for electromagnetic tunability: electrically, magnetically, chemically, thermally or optically (at microwaves) controllable materials, composites with conductive inclusions loaded by controllable elements like varactors or p-i-n diodes, utilization of electromagnetic non-linearity, etc. (see e.g. in [85]). However, one of the simplest mechanisms – mechanical deformation of the unit cell’s geometry – is rather weakly explored in the metamaterial science in spite of its high efficiency. Therefore, this topic was selected for the last chapter of this dissertation. Realization of the mechanical control is possible, e.g. with elastic polymers (elastomers), which can serve a host matrix for resonant inclusions. Elastomers substrates for planar MtMs (metasurfaces) represent a powerful tool for the mechanical control of electromagnetic properties. There are several examples of flexible MSs in different frequency ranges, see the review paper [86]. At optical frequencies stretching was used to modify the plasmonic response of the unit cell, shifting the resonance bands. Here, such types of design solutions as bow-tie nanoantennas [87], plasmonic nanospheres [88], and split-ring resonators [89] should be mentioned. At the microwave and terahertz ranges, split-ring resonators were also utilized [90,91] as well as more complicated designs based on modified metal crosses, slotted patches, and other similar resonant inclusions [92-94]. The main feature of these design solutions is that stretching changes the distance between two capacitively coupled parts of the resonant elements, which leads to a shift of the resonance i.e. to a noticeable change of the scattering at the resonance frequency of the non-stretched MS. However, the sensitivity to stretching, using this mechanism, is rather weak, because the resonant frequency is proportional to  $1/\sqrt{C}$ . Perspective applications of flexible MSs as remote (optical) sensors of stretching, called strain gauges (the strain and the stretching are related with the known Young modulus of the elastomer), would require a stronger

response to stretching, which should be easily detected in order to be contestable with the existing prototypes. Modern optical strain gauges are mainly based on two methods: diffraction gratings, which are attached to a specimen, and in which stretching increases the amount of diffraction lobes [95,96], and image-correlation measurements [97,98], based on the digitalization of optical images of the specimen before and after deformation. Both these techniques are rather complicated and result in quite expensive devices. Therefore, flexible MSs would be good candidates for prospective strain gauges if sufficient sensitivity of the reflection and/or transmission to the stretching is reached. Flexible MSs can also find other applications, e.g. can be used in prospective devices where the sensitivity to stretching is combined with other functionalities. In [V], the design solution of such multifunctional MS is presented.

#### 4.1 Design of a multifunctional metasurface

The concept of multifunctional MSs requires a more complicated mechanism of stretching sensitivity than simple capacitive coupling. The key idea developed in [V] is the engineering of MSs, in which not only the distance between individual inclusions is changed with stretching, but also their mutual orientation. This approach allows utilization of electromagnetic

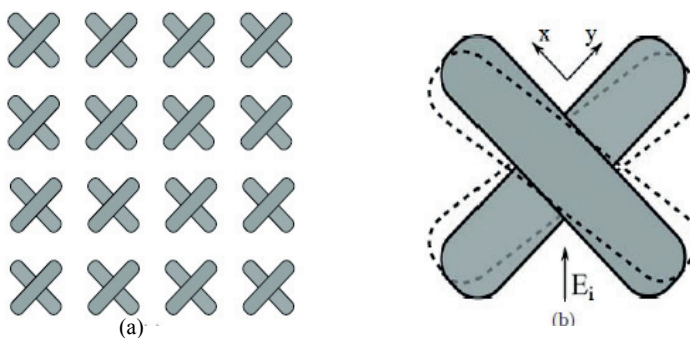


Fig 10 (a) - Double-array of metal stripes on elastic substrate. (b) - One unit cell, dashed lines show reorientation due to stretching.

effects, which are forbidden due to the symmetry restrictions, unless the strain is applied. The scheme of such a MS is shown in Fig.10.



The substrate of the MSs is polydimethylsiloxane (PDMS), providing the required elasticity as well high transparency in a wide frequency range. On the top and bottom of the PDMS film of thickness, 200  $\mu\text{m}$  planar metal stripes are deposited. The metal stripes have a length of 660  $\mu\text{m}$ , the width 130  $\mu\text{m}$ , and the thickness 200 nm. In fact, the size of the stripes and the substrate thickness define the operation frequency of the MS, which was chosen to be in the THz range. Of course, by the proper choice of geometrical parameters, the frequency can be altered in a very wide range, but the THz band has many advantages, among the most important being a simple and feasible fabrication by standard optical lithographic techniques.

Let us consider the normal incidence of a linearly polarized plane wave on the MSs with polarization as shown in Fig.10. It can be shown that the amplitudes of co- and cross-polarized components of reflected fields are as follows:

$$E_{co}^r = \frac{1}{2}R_0(1 + e^{j2kl}), \quad E_{cross}^r = \frac{1}{2}R_0(1 - e^{j2kl}) \quad (12)$$

Here,  $l$  is the thickness of the substrate,  $k$  is the wave number inside the substrate, and  $R_0$  is the amplitude of the reflection coefficient of a single grid of parallel stripes. For the thickness of the film equal to one-quarter of wavelength, the amplitude of the co-polarized reflected field is zero, and the structure works as a frequency-selective twist polarizer. If the stripes are at resonance, the transmission through the film is very small, and the power of the incident wave is effectively converted into a cross-polarized reflected

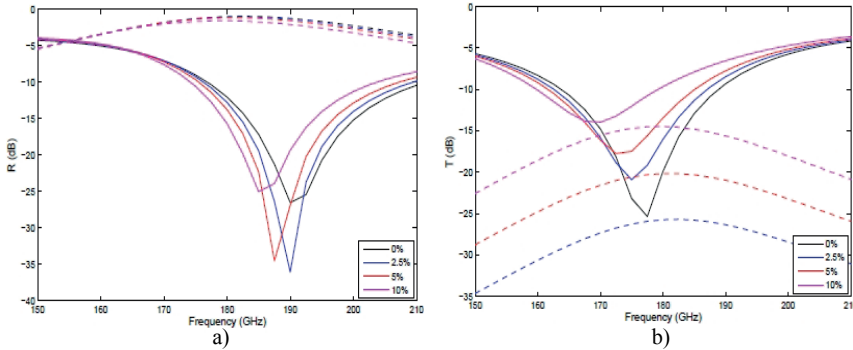


Fig. 11: (a) Reflection and (b) transmission coefficients for different magnitudes of stretching. Co- and cross-polarization components are shown by solid and dashed lines, respectively.

field. Away from the resonance, the MS weakly interacts with the incident field and the transmission prevails.

The mechanism of polarization rotation is similar to one used in [100]. In that work, the reflector twist-polarizer was realized by the grid of parallel wires on top of a metal screen. The distance between the grid and the screen was also  $\lambda_{eff}/4$ , leading to the compensation of the co-polarized term. The main difference of the design based on metal stripes is an off-resonance transparency allowing other functionalities, namely strain sensing.

Stretching of the MS of resonant stripes causes their reorientation and deteriorates the twist-polarization properties. However, this mechanism provides unusual dependence of the scattered field on stretching, shown in Fig.11. At 188 GHz, where the film thickness is equal to  $\lambda_{eff}/4.45$ , cross-polarization reflection is -2 dB, co-polarization is -27 dB. The twist-polarization mechanism works as predicted by eqs. (12), the difference of the operation frequency is related to the additional reactance of the resonant stripes. The resonance is rather broadband and the stretching only slightly reduces the twist-reflection effect. However, the strain substantially increases transmission in co-polarization and, moreover, leads to appearing of cross-polarization transmission. It happens because of the symmetry-break caused by the reorientation of the stripes due to stretching. Thus, strong sensitivity of both components of transmitted field on stretching allows perspective operation of the structure as a strain sensor, which is accompanied by the transformation of polarization of the reflected field, robust to the mechanical strain.

Another orientation of the MS, shown in Fig.12, also provides interesting

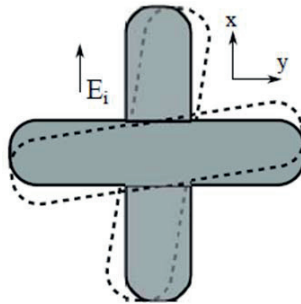


Fig. 12: Unit cell of the array, dashed lines show reorientation due to stretching.

dependence on stretching. In this case, there is no polarization transformation in the reflected field, and the amplitude of the co-polarized reflected field is very high independently to the applied strain. However, stretching leads to the excitation of the second array, which otherwise very weakly interacts with the incident field. Due to this effect, cross-polarized transmission is zero without strain; but even for 5%, stretching exceeds the co-polarized one. Such behavior is also perspective for sensing applications.

Of course the presented mechanism of polarization transformation in thin arrays is not unique. Among the known classical solutions, one can mention gyrotropic media, which, under applied high values of magnetic bias fields, can rotate polarization by 90 degrees. Another well-known method is the utilization of resonant chiral inclusions for polarization rotation. Plenty of design solutions of thin chiral MtMs have been presented in the literature recently: double-arrays of inclusions with chirality due to broken rotation symmetry [101,102], cholesteric structures [103], and optimal chiral polarization transformers [104] are among them. However, none of these designs are perspective for strain-sensing applications.

## **4.2 Fabrication and measurements**

Fabrication of double side arrays of metal stripes on the elastic film is a challenging task. The main problem is the necessity of the strip alignment from both sides with high accuracy and at the same time providing high electrical conductivity of the stripes. Ideally, it requires special equipment for formation of photoresist layers on flexible films and double-size alignment during exposure. Instead, in [V], the simple fabrication method was suggested as feasible with standard microfabrication facilities. In the first step, a 200- $\mu\text{m}$ -thick PDMS film was made using a Sylgard-184 silicon elastomer kit. Then, the separate shadow-mask was prepared from 4 silicon wafers by means of through etching in ICP-RIE, for which an aluminum mask was formed by standard optical lithography. The PDMS film was then put on a holder, and the shadow mask was fixed on the top of the film during a sputtering of 200 nm copper layer. In the next step, for sputtering

of the second array of metal stripes, a shadow mask was rotated 90 degrees and aligned at the other side of the film with respect to the first array.

The limitations of the process are connected with utilization of the thin elastic film. During attaching and detaching of the film from the holders, part of the film was subjected to stress, resulting in the broken periodicity of arrays. The other problem is a variation of the gap between the shadow mask and the film, leading to the distortion of the particle shape. These factors, together with high roughness of deposited copper, lead to the presence of substantial scattering and absorption losses, not taken into account in the numerical simulations. Despite the discussed drawbacks the suggested fabrication method allowed a rather simple fabrication of an optically large array with a size of  $7 \times 7 \text{ cm}^2$  and thickness much smaller than the operation wavelength.

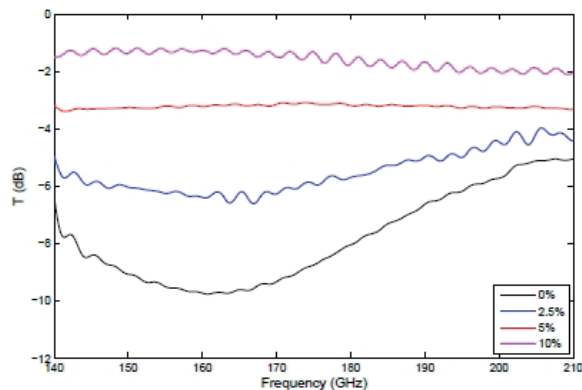


Fig. 13 Co-polarization transmission coefficient for different magnitudes of stretching

The film was installed in a sliding frame, which allowed for control of relative stretching and was put between two horn antennas with separate lenses for creating a normal incident plane wave. The sample allowed stretching up to 10% with restorable electromagnetic response. The transmission for co-polarization after filtering of fluctuations, due to multiple reflections in the measurement setup, is shown in Fig. 13.

The amplitude of the resonance is about 15 dB smaller than in the simulations, which is explained by the fabrication tolerances discussed earlier. At the same dependence on stretching and resonant frequency is close to the predictions. Without stretching, the resonance is -10 dB and

almost linearly changes up to -1.5 dB for 10% stretching. The level of cross-polarized transmission and co-polarized reflection was below the noise in measurement setup. Lack of the necessary equipment did not allow for measuring of the cross-polarized reflection and demonstration of polarization transformation properties experimentally.

### **4.3 Discussion and future research**

The suggested design solution combined polarization transformation properties with high sensitivity to the applied mechanical strain. The fabrication method allowed for the creation of optically big arrays by standard techniques, although the process is not without drawbacks, leading to higher losses and weaker resonant properties of the fabricated sample compared to theoretical predictions. However, our samples possess excellent linear sensitivity to strain, which is sufficient for sensing applications. At the same time, the improvement of fabrication issues is necessary and requires further studies. Improvement of the quality of the samples will allow measurements of the impact of strain to cross-polarized transmittance, and the modification of the measurement setup, which will allow measurements of the reflectance, is necessary for experimental validation of the twist-polarizing properties. Another important problem, for which a solution is needed for practical applications, is the interaction of the MS with the specimen, whose strain is measured. Undoubtedly, placing the MS on the specimen will affect the scattering properties of MS. This issue will be hopefully studied in our future works.

## 5. Conclusions

The research of this doctoral thesis is related to the field of MtMs, based on different types of resonant inclusions. It studies manifold physical phenomena in a very wide frequency range, from THz frequencies to the visible spectrum. The main goal of the work was the engineering of MtMs with new and extreme electromagnetic properties and their electromagnetic characterization.

The first part of the thesis is related to the concept of artificial magnetism and isotropic negative permittivity and permeability in the near-infrared and visible ranges. It was shown that the realization of such extreme material parameters at such high frequencies is complicated by many factors, among which Ohmic losses in plasmonic metals is the most essential. Several design solutions were proposed based on different types of complex-shaped resonant inclusions. The problem of isotropic negative permeability was solved by the utilization of spherical clusters of resonant plasmonic particles. The isotropic negative refractive index was obtained in the MtM consisting of core-shell metal-dielectric particles, combining plasmon electric and Mie magnetic resonances. The results were obtained theoretically and validated by full-wave numerical simulations, opening the way towards future practical implementations of the suggested design solutions.

The second part of the thesis is devoted to the characterization of planar and bulk MtMs. The discussion of the present homogenization methods revealed that the problem of proper characterization of MtMs is far from being fully solved in the modern literature. At first, it was shown in the work that the so-called Holloway-Kuester homogenization method is applicable for planar arrays of rather optically substantial resonant clusters of plasmonic nanoparticles, despite the fact that initially it had been developed for arrays of solid particles in the quasi-static approximation. Then, the new method of homogenization of bulk composites was suggested and applied for the bulk arrays of nanorings of plasmonic spheres. It was

shown that the method reveals the electromagnetic properties not covered by the standard quasi-static homogenization procedures.

The third part introduces the concept of multifunctional MSs for the THz frequency range. The suggested design allowed for the combination of polarization transformation properties with sensitivity to the applied strain. In addition to the theoretical and numerical studies, the new fabrication method was developed, allowing a rather simple creation of optically very large samples. Despite the revealed fabrication tolerances, the samples experimentally demonstrated a high sensitivity to stretching in the transmission coefficient for the co-polarized field. The work is promising for future strain-sensing applications, although requires further studies directed towards the improvement of the fabrication method and solving some specific practical problems.

The MtM science is a very rapidly developing area of human knowledge, despite being very young. The research topics studied in the thesis are very up-to-date, and new results are published yearly. In general, theoretical studies of MtMs not only reveal new remarkable electromagnetic properties, not normally met in nature, they also push forward different branches of MtM science, resulting in the progress of the entire field. Theoretical studies of MtM for optical frequencies urge the nanomaterial science, leading to the development of new nanofabrication methods for the creation of composites, which were unattainable earlier. The theoretical studies of plasmonic composites presented in the thesis were conducted in close contact with our partners from the METACHEM project, which in their turn made important developments in the nanofabrication field. Our results of MtM characterization, along with the finding of many other research groups, allowed for a better understanding of the physical phenomena demonstrated by MtMs. Finally, the last results on the multifunctional MS attracted attention to the realization of flexibility and elasticity for the THz MtMs, an area rather weakly explored in the modern literature.

## 6. Summary of publications

### **Publication I: “Negative effective permeability at optical frequencies produced by rings of plasmonic dimers”**

This paper suggests a design solution for creating the artificial magnetic response of nanostructured metamaterials in the optical frequency range. This design solution is a modification of the known effective rings formed by plasmonic nanospheres located at the corners of a regular polygon. Instead of nanospheres the plasmonic dimers (pairs of intersecting spheres) are utilized, which allows stronger robustness to Ohmic absorption in silver. It is theoretically shown that the suggested metamaterial possesses negative permeability at the edge between the near-infrared and visible ranges.

### **Publication II: “Electromagnetic characterization of planar and bulk metamaterials: A theoretical study”**

In the first part of the paper, the applicability of the so-called Holloway-Kuester characterization method for metasurface of resonant clusters of plasmonic particles is studied. It is shown that despite the fact that the approach initially was developed for arrays of solid particles in the quasi-static approximation, it is also applicable for bilayers of plasmonic spheres for prediction of scattering parameters and extraction of polarizabilities. In the second part, the original dynamic approach is suggested, which allows extraction of the effective material parameters of bulk lattices from the reflection and transmission coefficients of a single generic metasurface. The results of this retrieval are compared with the results of an alternative method based on the quasi-static homogenization model. The method reveals the electromagnetic properties not covered by the standard quasi-static homogenization procedures.



**Publication III: “Isotropic negative effective permeability in the visible range produced by clusters of plasmonic triangular nanoprisms”**

In this paper, a design solution of metamaterial made of raspberry-like clusters of silver triangular nanoprisms is suggested. The magnetic polarizability of the cluster is estimated by two independent methods, allowing optimization of the geometry for the higher resonant response. It is shown that the design theoretically allows isotropic negative effective permeability in the visible range taking into account real dissipative losses in silver.

**Publication IV: “Isotropic negative refractive index at near infrared”**

In the paper, the design solution of metamaterial composed of core-shell metal-dielectric spherical particles is suggested and studied. The polarizabilities of individual particles are calculated by analytical Mie theory and independently extracted from numerical simulations. According to both approximate analytical theory and simulations, metamaterial possesses an isotropic negative refractive index in the near-infrared frequency range. The effect of negative refraction is confirmed by the full-wave simulations of the Gaussian beam, diverted by a metamaterial prism.

**Publication V: “Multifunctional stretchable metasurface for the THz range”**

A metamaterial suggested in the paper consists of resonant metal stripes put on two sides of an elastic polymer film and allows for the combination of polarization transformation properties with sensitivity to the applied strain. The design is studied theoretically, numerically, and experimentally. For the last purpose, an original fabrication method is developed, allowing a rather simple creation of optically very large samples. The fabricated sample experimentally demonstrates a high sensitivity to stretching in the transmission coefficient for the co-polarized field.

## Bibliography

- [1] V. G. Veselago, "The electrodynamics of substances with simultaneously negative values of  $\epsilon$  and  $\mu$ ", *Sov. Phys. Usp.*, vol. 10, no. 4, pp. 509-514, Jan. 1968.
- [2] J. B. Pendry, "Negative refraction makes perfect lens", *Phys. Rev. Lett.*, vol. 85, no.18, pp. 3966-3969, Oct. 2000.
- [3] A. Grbic and G. V. Eleftheriades, "Overcoming the Diffraction Limit with a Planar Left-Handed Transmission-Line Lens", *Phys. Rev. Lett.*, vol. 92, no. 11, p. 117403, Mar. 2004.
- [4] R. A. Shelby, D. R. Smith and S. Schultz, "Experimental verification of a negative index of refraction", *Science*, vol. 292, no. 5514, pp. 77-79, Apr. 2001.
- [5] J. Zhou, Th. Koschny and C. M. Soukoulis, "Magnetic and electric excitation of split ring resonators", *Opt. Express.*, vol. 15, no. 26, pp. 17881-17890, Dec. 2007.
- [6] Ph. Gay-Balmaz, O. J. F. Martin, "Electromagnetic resonances in individual and coupled split-ring resonators", *J. Appl. Phys.*, vol. 92, no. 5, pp. 2929-2936, Sep. 2002.
- [7] K. Aydin, I. Bulu, K. Guven, M. Kafesaki, C. M Soukoulis and E. Ozbay, "Investigation of magnetic resonances for different SRR parameters and designs", *New J. Phys.*, vol. 7, no. 168, pp. 1-13, Aug. 2005.
- [8] C. M. Soukoulis, T. Koschny, J. Zhou, M. Kafesaki, and E. N. Economou, "Magnetic response of split ring resonators at terahertz frequencies", *Phys. Status Solidi B*, vol. 244, no. 4, pp. 1181-1187, Mar. 2007.
- [9] G. Dolling, C. Enkrich, M. Wegener, J. F. Zhou, C. M. Soukoulis and S. Linden, "Cut-wire pairs and plate pairs as magnetic atoms for optical metamaterials", *Opt. Lett.*, vol. 30, no. 23, pp. 3198-3200, Dec. 2005.
- [10] C. R. Simovski and B. Sauviac, "Toward creating isotropic microwave composites with negative refraction", *Radio Sci.*, vol. 39,

- no. 2, p. RS2014, Apr. 2004.
- [11] J. D. Baena, L. Jelinek, R. Marqués and J. Zehentner, “Electrically small isotropic three-dimensional magnetic resonators for metamaterial design”, *Appl. Phys. Lett.*, vol. 88, no. 13, p. 134108, Mar. 2006.
  - [12] J. Zhou, Th. Koschny, M. Kafesaki, E. N. Economou, J. B. Pendry and C. M. Soukoulis, “Saturation of the magnetic response of splitting resonators at optical frequencies”, *Phys. Rev. Lett.*, vol 95, no. 22, p. 223902, Nov. 2005.
  - [13] G. Dolling, C. Enkrich, M. Wegener, C. M. Soukoulis and S. Linden, “Simultaneous Negative Phase and Group Velocity of Light in a Metamaterial”, *Science*, vol. 312, no. 5775, pp. 892-894, May 2006.
  - [14] M. Kafesaki, I. Tsiapa, N. Katsarakis, Th. Koschny, C. M. Soukoulis, and E. N. Economou, “Left-handed metamaterials: The fishnet structure and its variations”, *Phys. Rev. B*, vol. 75, no. 23, p. 235114, June 2007.
  - [15] J. Yang, C. Sauvan, H. T. Liu, and P. Lalanne, “Theory of Fishnet Negative-Index Optical Metamaterials”, *Phys. Rev. Lett.*, vol. 107, no. 4, p. 043903, July 2011.
  - [16] A. Alù, A. Salandrino and N. Engheta, “Negative effective permeability and left-handed materials at optical frequencies”, *Opt. Express*, vol. 14, no. 4, pp. 1557-1567, Feb. 2006.
  - [17] C. R. Simovski and S. A. Tretyakov, “Model of isotropic resonant magnetism in the visible range based on core-shell clusters”, *Phys. Rev. B*, vol. 79, no. 4, p. 045111, Jan. 2009.
  - [18] A. Alù and N. Engheta, “Dynamical theory of artificial optical magnetism produced by rings of plasmonic nanoparticles”, *Phys. Rev. B*, vol. 78, no. 5, p. 085112, Aug. 2008.
  - [19] P. B. Johnson and R. W. Christy, “Optical Constants of the Noble Metals”, *Phys. Rev. B*, vol. 6, no. 12, pp. 4370-4379, Dec. 1972.
  - [20] I. Romero, J. Aizpurua, G. W. Bryant and F. J. Garcia de Abajo, “Plasmons in nearly touching metallic nanoparticles: singular response in the limit of touching dimers”, *Opt. Express*, vol 14, no.

- 21, pp. 9988-9999, Oct. 2006.
- [21] M. Pitkonen, "Polarizability of the dielectric double-sphere", *J. Math. Phys.*, vol. 47, no. 10, p. 102901, Oct. 2006.
- [22] D. ten Bloemendal, P. Ghenuche, R. Quidant, I. G. Cormack, P. Loza-Alvarez, and G. Badenes, "Local Field Spectroscopy of Metal Dimers by TPL Microscopy", *Plasmonics*, vol. 1, no.1, pp. 41-44, Mar. 2006.
- [23] K. L. Shuford, M. A. Ratner and G. C. Schatz, "Multipolar Excitation in Triangular Nanoprisms", *J. Chem. Phys.*, vol. 123, no. 11, p. 114713, Sep. 2005.
- [24] L. J. Sherry, R. Jin, C. A. Mirkin, G. C. Schatz and R. P. Van Duyne, "Localized surface plasmon resonance spectroscopy of single silver triangular nanoprisms", *Nano Lett.*, vol. 6, no. 9, pp. 2060-2065, Jul. 2006.
- [25] M. Rang, A. C. Jones, F. Zhou, Z. Li, B. J. Wiley, Y. Xia and M. B. Raschke, "Optical near-field mapping of plasmonic nanoprisms", *Nano Lett.*, vol. 8, no. 10, pp. 3357-3363, Sep. 2008.
- [26] C. F. Bohren, D. R. Huffman, *Absorption and Scattering of Light by Small Particles*. John Wiley & Sons, 2008.
- [27] C. L. Holloway, E. F. Kuester, J. Baker-Jarvis and P. Kabos, "A double negative (DNG) composite medium composed of magnetodielectric spherical particles embedded in a matrix", *IEEE Trans. Ant. Prop.*, vol. 51, no. 10, pp. 2596-2603, Oct. 2003.
- [28] C. R. Simovski, "Analytical modelling of double-negative composites", *Metamaterials*, vol. 2, no 4, pp. 169-185, Dec. 2008.
- [29] S. Ghadarghadr and H. Mosallaei, "Dispersion Diagram Characteristics of Periodic Array of Dielectric and Magnetic Materials Based Spheres", *IEEE Trans. Ant. Prop.*, vol. 57, no. 1, pp. 149-160, Jan. 2009.
- [30] M. Wheeler, J. Aitchison and M. Mojahedi, "Coated nonmagnetic spheres with a negative index of refraction at infrared frequencies", *Phys. Rev. B*, vol. 73, no. 4, p. 045105, Jan. 2006.
- [31] E. Hao, S. Li, R. C. Bailey, S. Zou, G. C. Schatz and J. T. Hupp, "Optical Properties of Metal Nanoshells", *J. Phys. Chem. B*, vol.

- 108, no. 4, pp. 1224-1229, Jan. 2004.
- [32] A. O. Pinchuk and G. C. Schatz, "Collective surface plasmon resonance coupling in silver nanoshell arrays" *Appl. Phys. B*, vol. 93, no. 1, pp. 31-38, Aug. 2008.
- [33] S. Tretyakov, *Analytical Modeling in Applied Electromagnetics*. Norwood, MA: Artech House, 2003.
- [34] R. Paniagua-Domínguez, F. López-Tejeira, R. Marqués and J. A. Sánchez-Gil, "Metallo-dielectric core-shell nanospheres as building blocks for optical three-dimensional isotropic negative-index metamaterials", *New J. Phys.*, vol. 13, no. 12, p. 123017, Dec 2011.
- [35] R. Paniagua-Domínguez, D. R. Abujetas and Sánchez-Gil, "Ultra low-loss, isotropic optical negative-index metamaterial based on hybrid metal-semiconductor nanowires", *Scien. Reports*, vol. 3, p. 1507, Mar. 2013.
- [36] S. N. Sheikholeslami, H. Alaeian, A.L. Koh, and J. A. Dionne, "A Metafluid Exhibiting Strong Optical Magnetism", *Nano Lett.*, vol. 13, no. 9, pp. 4137-4141, Aug. 2013.
- [37] J. Angly, A. Iazzolino, J.-B. Salmon, J. Leng, S. P. Chandran, V. Ponsinet, A. Désert, A. Le Beulze, S. Mornet, M. Tréguer-Delapierre and M. A. Correa-Duarte, "Microfluidic-Induced Growth and Shape-Up of Three-Dimensional Extended Arrays of Densely Packed Nanoparticles", *ACS Nano*, vol. 7, no. 8, pp. 6465-6477, July 2013.
- [38] Y. Yao, M. T. McDowell, I. Ryu, H. Wu, N. Liu, L. Hu, W. D. Nix and Y. Cui, "Interconnected Silicon Hollow Nanospheres for Lithium-Ion Battery Anodes with Long Cycle Life", *Nano Lett.*, vol. 11, no. 7, pp. 2949-2954, June 2011.
- [39] K. Aslan, M. Wu, J. R. Lakowicz and C. D. Geddes, "Fluorescent Core-Shell Ag@SiO<sub>2</sub> Nanocomposites for Metal-Enhanced Fluorescence and Single Nanoparticle Sensing Platforms", *J. Am. Chem. Soc.*, vol. 129, no. 6, pp. 1524-1525, Jan. 2007.
- [40] Y. Zhou, Y. Liu, J. Cheng and Y. Lo, "Bias dependence of sub-bandgap light detection for coreshell silicon nanowires", *Nano Lett.*, vol. 12, no. 11, p. 5929-593, Oct. 2012.
- [41] R. E. Algra, M. Hocevar, M. A. Verheijen, I. Zardo, G. G. W.

- Immink, W. J. P. van Enkevort, G. Abstreiter, L. P. Kouwenhoven, E. Vlieg and E. P. A. M. Bakkers, “Crystal structure transfer in core/shell nanowires”, *Nano Lett.*, vol. 11, no. 4, pp. 1690–1694, Mar. 2011.
- [42] C. R. Simovski, “On electromagnetic characterization and homogenization of nanostructured metamaterials”, *J. Optics*, vol. 13, no. 1, p. 013001, Nov. 2010.
- [43] J. C. Maxwell Garnett, “Colours in metal glasses and in metallic films”, *Phil. Trans. R. Soc. London A*, vol. 203, pp. 385-420, June 1904.
- [44] D. Polder, J. H. van Santeen, “The effective permeability of mixtures of solids”, *Physica*, vol. 12, no. 5, pp. 257–271, Aug. 1946.
- [45] G. Shvets and Y. A. Urzhumov, “Electric and magnetic properties of sub-wavelength plasmonic crystals”, *J. Opt. A: Pure Appl. Opt.*, vol. 7, no. 2, pp. S23-S31, Jan. 2005.
- [46] Y. A. Urzhumov and G. Shvets, “Optical magnetism and negative refraction in plasmonic metamaterials”, *Solid State Commun.*, vol. 146, no. 5, pp. 208-220, May 2008.
- [47] G. Bouchitte, C. Bourel and D. Felbacq, “Homogenization of the 3D Maxwell system near resonances and artificial magnetism”, *C. R. Acad. Sci. Paris I*, vol.347, no. 9, pp. 571-576, May 2009.
- [48] S. Guenneau, F. Zolla and A. Nicolet, “Homogenization of three-dimensional photonic crystals with heterogeneous permittivity and permeability”, *Waves Random Complex Media*, vol. 17, no. 4, pp. 653-697, Oct. 2007.
- [49] J. B. Pendry, A. J. Holden, D. J. Robbins and W. J. Stewart, “Magnetism from conductors and enhanced nonlinear phenomena”, *IEEE Trans. Microwave Theory Tech.*, vol. 47, no. 11, pp. 2075-2084, Nov. 1999.
- [50] M. G. Silveirinha, “Metamaterial homogenization approach with application to the characterization of microstructured composites with negative parameters”, *Phys. Rev. B*, vol. 75, no. 11, p. 115104, Mar. 2007.
- [51] M. G. Silveirinha, “Generalized Lorentz–Lorenz formulas for

- microstructured materials”, *Phys. Rev. B*, vol. 76, no. 24, p. 245117, Dec. 2007.
- [52] M. G. Silveirinha, “Additional boundary conditions for nonconnected wire media”, *New J. Phys.*, vol. 11, p. 113016, Nov. 2009.
- [53] A. M. Nicolson and G. F. Ross, “The measurement of the intrinsic properties of materials by time-domain techniques”, *IEEE Trans. Instrum. Meas*, vol. 17, no. 4, pp. 377-382, Nov. 1970.
- [54] W. W. Weir, “Automatic measurement of the complex dielectric constant and permeability at microwave frequencies”, *Proc. IEEE*, vol 62, no. 1, pp. 33-36, Jan. 1974.
- [55] D. R. Smith, D. C. Vier, T. Koschny, and C. M. Soukoulis, “Electromagnetic parameter retrieval from inhomogeneous metamaterials”, *Phys. Rev. E*, vol. 71, no. 3, p. 036617, Mar. 2005.
- [56] S. O’Brien and J. B. Pendry, “Magnetic activity at infrared frequencies in structured metallic photonic crystals”, *J. Phys. Condens. Matter*, vol. 14, no. 25, pp. 6383-6394, June 2002.
- [57] D. R. Smith, S. Schultz, P. Markos and C. Soukoulis, “Determination of effective permittivity and permeability of metamaterials from reflection and transmission coefficients”, *Phys. Rev. B*, vol. 65, no. 19, p. 195104, Apr. 2002.
- [58] T. Koschny, P. Markos, D.R. Smith and C.M. Soukoulis, “Resonant and anti-resonant frequency dependence of the effective parameters of metamaterials”, *Phys. Rev. E*, vol. 58, no. 6, p. 065602, Dec. 2003.
- [59] S. O’Brien, J.B. Pendry, “Photonic band gap effects and magnetic activity of dielectric composites”, *J. Phys.: Condens. Matter*, vol. 14, no. 15, pp. 4035-4044, Apr. 2002.
- [60] N. Katsarakis, T. Koschny, M. Kafesaki, E. N. Economou, E. Ozbay and C. M. Soukoulis., “Left- and right-handed transmission peaks near the magnetic resonance frequency in composite metamaterials”, *Phys. Rev. B*, vol. 70, no. 20, p. 201101, Nov. 2004.
- [61] T. Koschny, M. Kafesaki, E. N. Economou and C. M. Soukoulis, “Effective medium theory of left-handed materials”, *Phys. Rev. Lett.*,

- vol. 93, no. 10, p. 107402, Sep. 2004.
- [62] U. K. Chettiar, A. V. Kildishev, T. A. Klar and V. M. Shalaev, “Negative index metamaterial combining magnetic resonators with metal films shape”, *Opt. Express*, vol. 30, no. 17, pp. 7872-7877, Aug. 2006.
- [63] G. Dolling, M. Wegener and S. Linden, “Realization of a three-functional-layer negative-index photonic metamaterial”, *Opt. Lett.*, vol. 32, no. 5, pp. 551-553, Mar. 2007.
- [64] V. M. Shalaev, W. Cai, U. K. Chettiar, H.-K. Yuan, A. K. Sarychev, V. P. Drachev and A. V. Kildishev, “Negative index of refraction in optical metamaterials”, *Opt. Lett.*, vol. 30, no. 24, pp. 3356-3358, Dec. 2005.
- [65] G. Dolling, M. Wegener, C. Soukoulis and S. Linden, “Negative-index metamaterial at 780 nm wavelength”, *Opt. Lett.*, vol. 32, no. 1, pp. 53-55, Jan. 2007.
- [66] J. D. Jackson, *Classical Electrodynamics 3rd edn.* New York: Wiley, 1999.
- [67] M. Born and K. Huang, *Dynamic Theory of Crystalline Lattices.* Oxford: Oxford University Press, 1954
- [68] C. R. Simovski, “On material parameters of metamaterials”, *Opt. Spectrosc.*, vol. 107, no. 5, pp. 726-753, Nov. 2009.
- [69] A. N. Grigorenko, A. K. Geim, H. F. Gleeson, Y. Zhang, A. A. Firsov, I. Y. Khrushchev and J. Petrovic, “Nanofabricated media with negative permeability at visible frequencies”, *Nature*, vol. 438, pp. 335-338, Sep. 2005.
- [70] A. N. Grigorenko, “Negative refractive index in artificial metamaterials”, *Opt. Lett.*, vol. 31, no. 16, pp. 2483-2485, Aug. 2006.
- [71] S. Linden, C. Enkrich, M. Wegener, J. F. Zhou, T. Koschny and C. M. Soukoulis, “Magnetic response of metamaterials at 100 THz”, *Science*, vol. 306, no. 5700, pp. 1351-1353, Nov. 2004.
- [72] S. Zhang, W. Fan, N. C. Panoiu, K. M. Malloy, R. M. Osgood and S. R. J. Brueck, “Experimental demonstration of near-infrared negative-index metamaterials” *Phys. Rev. Lett.*, vol. 95, no. 13, p.



137404, Sep. 2005.

- [73] T. J. Yen, W. J. Padilla, N. Fang, D. C. Vier, D. R. Smith, J. B. Pendry and D. N. Basov, “Terahertz magnetic response from artificial materials”, *Science*, vol. 303, no. 5663, pp. 1494-1496, Mar. 2004.
- [74] C. Enkrich, S. Linden, M. Wegener, S. Burger, L. Zschiedrich, F. Schmidt, J. Zhou, T. Koschny and C. M. Soukoulis, “Magnetic metamaterials at telecommunication and visible frequencies”, *Phys. Rev. Lett.*, vol. 95, no. 20, p. 203901, Nov. 2005.
- [75] P. Alitalo, A. E. Culhaoglu, C. R. Simovski, and S. A. Tretyakov, “Experimental study of anti-resonant behavior of material parameters in periodic and aperiodic composite materials”, *J. Appl. Phys.*, vol. 113, no. 22, p. 224903, June 2013.
- [76] A. Alù, “Restoring the physical meaning of metamaterial constitutive parameters”, *Phys. Rev. B*, vol. 83, no. 8, p. 081102, Feb. 2011.
- [77] C. R. Simovski, S. A. Tretyakov, “Local constitutive parameters of metamaterials from an effective-medium perspective”, *Phys. Rev. B*, vol. 75, no. 19, p. 195111, May 2007.
- [78] C. R. Simovski, “Bloch material parameters of magneto-dielectric metamaterials and the concept of Bloch lattices”, *Metamaterials*, vol. 1, no. 2, pp. 62-80, Dec. 2007.
- [79] E. F. Kuester, M. A. Mohamed, M. Piket-May and C. L. Holloway, “Averaged transition conditions for electromagnetic fields at a metafilm”, *IEEE Trans. Antennas Propag.*, vol. 51, no. 10, pp. 2641-2651, Oct. 2003.
- [80] C. L. Holloway, A. Dienstfrey, E. F. Kuester, J. F. O’Hara, A. K. Azad and A. J. Taylor, “A discussion on the interpretation and characterization of metafilms/metasurfaces: The two-dimensional equivalent of metamaterials”, *Metamaterials*, vol. 3, no. 2, pp. 100-112, Oct. 2009.
- [81] A. Alù, “First-principles homogenization theory for periodic metamaterials”, *Phys. Rev. B*, vol. 84, no. 7, p.075153, Aug. 2011.
- [82] S. Kim, E. F. Kuester, C. L. Holloway, A. D. Sher and J. Baker-

- Jarvis, "Boundary effects on the determination of metamaterial parameters from normal incidence reflection and transmission measurements", *IEEE Trans. Antennas Propag.*, vol. 59, no. 6, pp. 2226-2240, June 2011.
- [83] A. P. Vinogradov, A. I. Ignatov, A. M. Merzlikin, S. A. Tretyakov and C. R. Simovski, "Additional effective medium parameters for composite materials (excess surface currents)", *Opt. Express*, vol. 19, no. 7, pp. 6699-6704, Mar. 2011.
- [84] P. Drude, *The Theory of Optics 3d ed.* Dover, London, 1959.
- [85] J. P. Turpin, J. A. Bossard, K. L. Morgan, D. H. Werner, P. L. Werner, "Reconfigurable and Tunable Metamaterials: A Review of the Theory and Applications", *Int. J. Ant. and Prop.*, 2014, early access.
- [86] J. J. Yang, M. Huang, H. Tang, J. Zeng and L. Dong, "Metamaterial Sensors", *Int. J. Ant. and Prop.*, vol. 2013, Article ID 637270, 2013.
- [87] S. Aksu, M. Huang, A. Artar, A. A. Yanik, S. Selvarasah, M. R. Dokmeci and H. Altug, "Flexible Plasmonics on Unconventional and Nonplanar Substrates", *Adv. Mater.*, vol. 23, no. 38, pp. 4422-4430, Oct. 2011.
- [88] X. Zhu, S. Xiao, L. Shi, X. Liu, J. Zi, O. Hansen and N. A. Mortensen, "A stretch-tunable plasmonic structure with a polarization-dependent response", *Opt. Express*, vol. 20, no. 5, pp. 5237-5242, Feb. 2012.
- [89] I. M. Pryce, K. Aydin, Y. A. Kelaita, R. M. Briggs and H. A. Atwater, "Highly Strained Compliant Optical Metamaterials with Large Frequency Tunability", *Nano Lett.*, vol. 10, no. 10, pp. 4222-4227, Sep. 2010.
- [90] E. Ekmekci and G. Turhan-Sayan, "Metamaterial Sensor Applications Based on Broadside-Coupled SRR and VShaped Resonator Structures" in *Proc. 2011 IEEE Int. Symp. Ant. and Prop. (APSURSI)*, pp. 1170-1172, July 2011.
- [91] H. Tao, A. C. Strikwerda, K. Fan, C. M. Bingham, W. J. Padilla, X. Zhang and R. D. Averitt, "Terahertz metamaterials on free-standing highly-flexible polyimide substrates", *J. Phys. D.: Appl. Phys.*, vol.

- 41, no. 23, p. 232004, Nov. 2008.
- [92] J. Li, Ch. M. Shah, W. Withayachumnankul, B. S.-Y. Ung, A. Mitchell, Sh. Sriram, M. Bhaskaran, Sh. Chang and D. Abbott, “Flexible terahertz metamaterials for dual-axis strain sensing”, *Opt. Lett.*, vol. 38, no. 12, pp. 2104-2106, June 2013.
- [93] G. Kenanakis, N.-H. Shen, Ch. Mavidis, N. Katsarakis, M. Kafesaki, C. M. Soukoulis and E. N. Economou, “Microwave and THz sensing using slab-pair-based metamaterials”, *Physica B*, vol. 407, no. 20, pp. 4070-4074, Oct. 2012.
- [94] R. Melik, E. Unal, N. K. Perkgoz, B. Santoni, D. Kamstock, Ch. Puttlitz and H. V. Demir, “Nested Metamaterials for Wireless Strain Sensing”, *IEEE J. Of Sel. Top. In Quant. Electr.*, vol. 16, no. 2, pp. 450-458, Mar.-Apr. 2010.
- [95] T. R. Pryor and W. P. T. North, “The diffractographic strain gage”, *Exp. Mech.*, vol. 11, no. 12, pp. 565-568, Dec. 1971.
- [96] A. Asundi and B. Zhao, “Optical strain sensor using position-sensitive detector and diffraction grating: error analysis”, *Opt. Eng.*, vol. 39, no. 6, pp. 1645-1651, June 2000.
- [97] R. Rotinat, R. Tie, V. Valle and J. C. Dupre, “Three optical procedures for local large-strain measurements”, *Strain*, vol. 37, no. 3, pp. 89-98, Aug. 2001.
- [98] J. Tyson, T. Schmidt and K. Galanulis, “Biomechanics Deformation and Strain Measurement with 3D Image Correlation Photogrammetry”, *Exp. Tech.*, vol. 26, no. 5, pp. 39-42, Sep. 2002.
- [99] B. Pan, K. Qian, H. Xie and A. Asundi, “Two-dimensional digital image correlation for in-plane displacement and strain measurements review”, *Meas. Science and Tech.*, vol. 20, no. 6, p. 062001, Apr. 2009.
- [100] G. L. Josefsson, “Wire polarizers for microwave antenna”, *Technical Report No. 81 Chalmers Univ. Tech.* 1978.
- [101] A. V. Rogacheva, V. A. Fedotov, A. S. Schwanecke and N. I. Zheludev, “Giant Gyrotropy due to Electromagnetic Field Coupling in a Bilayered Chiral Structure”, *Phys. Rev. Lett.*, vol. 97, no. 17, p. 177401, Oct. 2006.

- [102] Y. Ye and S. He, “90 degree polarization rotator using a bilayered chiral metamaterial with giant optical activity”, *Appl. Phys. Lett.*, vol. 96, no. 20, p. 203501, May 2010.
- [103] Y. Svirko, N. Zheludev and M. Osipov, “Layered chiral metallic microstructures with inductive coupling”, *Appl. Phys. Lett.*, vol. 78, no. 4, pp. 498-500, Jan. 2001.
- [104] T. Niemi, A. O. Karilainen and S. A. Tretyakov, “Synthesis of Polarization Transformers”, *IEEE Trans. Ant. and Prop.*, vol. 61, no. 6, pp. 3102-3111, June 2013.

The thesis is devoted to the field of metamaterials - effectively continuous artificial composites with advantageous electromagnetic properties not normally met in nature. It studies manifold physical phenomena in a very wide frequency range, from THz frequencies to the visible spectrum. The main goal of the work is the engineering of metamaterials with new and extreme electromagnetic properties and their electromagnetic characterization. The thesis is divided into three research problems. The first part of the thesis is related to the concept of artificial magnetism and isotropic negative permittivity and permeability in the near-infrared and visible ranges. The second part of the thesis is devoted to the characterization of planar and bulk metamaterials. The third part introduces the concept of multifunctional metasurfaces for the THz frequency range. The methods being used are mainly analytical and semi-analytical modeling, verified by full-wave numerical simulations of Maxwell's equations and experimental measurements.



ISBN 978-952-60-5658-6  
ISBN 978-952-60-5659-3 (pdf)  
ISSN-L 1799-4934  
ISSN 1799-4934  
ISSN 1799-4942 (pdf)

**Aalto University**  
**School of Electrical Engineering**  
Department of Radio Science and Engineering  
[www.aalto.fi](http://www.aalto.fi)

**BUSINESS +  
ECONOMY**

**ART +  
DESIGN +  
ARCHITECTURE**

**SCIENCE +  
TECHNOLOGY**

**CROSSOVER**

**DOCTORAL  
DISSERTATIONS**